



**HAL**  
open science

## Influence of Maillard reaction and temperature on functional, structure and bioactive properties of fish gelatin films

Hela Kchaou, Nasreddine Benbettaieb, Mourad Jridi, Moncef Nasri, Frédéric Debeaufort

► **To cite this version:**

Hela Kchaou, Nasreddine Benbettaieb, Mourad Jridi, Moncef Nasri, Frédéric Debeaufort. Influence of Maillard reaction and temperature on functional, structure and bioactive properties of fish gelatin films. *Food Hydrocolloids*, 2019, 97, pp.105196. 10.1016/j.foodhyd.2019.105196 . hal-02173248

**HAL Id: hal-02173248**

**<https://u-bourgogne.hal.science/hal-02173248>**

Submitted on 25 Oct 2021

**HAL** is a multi-disciplinary open access archive for the deposit and dissemination of scientific research documents, whether they are published or not. The documents may come from teaching and research institutions in France or abroad, or from public or private research centers.

L'archive ouverte pluridisciplinaire **HAL**, est destinée au dépôt et à la diffusion de documents scientifiques de niveau recherche, publiés ou non, émanant des établissements d'enseignement et de recherche français ou étrangers, des laboratoires publics ou privés.



Distributed under a Creative Commons Attribution - NonCommercial 4.0 International License



23 **Abstract**

24 This study aims to assess the effect of heating temperatures on structure, physicochemical and  
25 antioxidant properties of fish gelatin films crosslinked by the temperature and/or with glucose  
26 by the Maillard reaction. Glucose was incorporated at a 0.5 glucose/lysine molar ratio into the  
27 fish gelatin film forming solutions. The products of the Maillard reaction were generated by  
28 heating the films during 24 h in a temperature range of 90-130 °C. An enhancement of some  
29 films properties was obtained after the induction of the Maillard reaction. Indeed, the water  
30 solubility and wettability were reduced. On the contrary, a rise of color intensity, UV-barrier  
31 property, radical scavenging activities and iron reducing effects was observed. These  
32 enhancements occurred also without glucose addition thanks to the heating treatment, but to  
33 a lesser extent. In addition, an increase of thermal stability due to structural changes was  
34 revealed by means of XRD, TGA and DSC analyses. As evidenced by the different  
35 experiments used for the determination of the antioxidant activity (DPPH• and ABTS free  
36 radicals scavenging activity, reducing power and β-carotene bleaching inhibition) the  
37 antioxidant activity of films containing glucose displayed an optimum after being treated at 90  
38 °C. On the contrary, it decreased or kept constant at higher temperatures, probably due to the  
39 degradation or further stages of Maillard reactions. Moreover, the thermal treatment alone ( $T$   
40  $\geq 100$  °C) can be a useful tool for enhancing the antioxidant activity of gelatin films. Finally,  
41 the Maillard reaction has a good potential to induce and generate bioactive compounds in  
42 gelatin films for food protection.

43

44 **Keywords:** fish gelatin; thermal treatment; Maillard reaction; crosslinking; physicochemical,  
45 thermal and structural properties; antioxidant activity.

## 46 **1. Introduction**

47 Nowadays, biodegradable films show a high interest in research and industrial fields as an  
48 alternative to synthetic packaging based on petrochemical sources, which are considered as a  
49 major cause of environmental pollution. Thus, different polymers have been used for film  
50 preparation such as proteins and polysaccharides. Amongst biodegradable films, protein-  
51 based-films have been widely studied for their physico-chemical and structural properties.  
52 Gelatin is a protein derived from collagen by hydrolysis, the primary protein component of  
53 animal connective tissues, which includes skin and tendon (Poppe, 1997). Gelatin is widely  
54 used by various industries because of its functional and technological properties. Fish gelatins  
55 have been equally extensively studied for their good film forming ability leading to produce  
56 transparent, colorless, water-soluble, highly stretchable and biodegradable films (Alfaro,  
57 Balbinot, Weber, Tonial, & Machado-Lunkes, 2015). However, due to their high hydrophilic  
58 amino acid content, films based on gelatin showed high brittleness and moisture sensitivity,  
59 which limit their applications (Etxabide, Urdanpilleta, de la Caba, & Guerrero, 2016; Liu et  
60 al., 2016). Therefore, the heating process could be a promising alternative to overcome the  
61 problems associated with the hydrophilic character of hydrocolloid-based films (Rivero,  
62 García& Pinotti, 2012). Heating proteins in the presence of a reducing sugar is a well-known  
63 method of crosslinking based on the Maillard reaction.

64 The Maillard reaction (MR), or non-enzymatic browning reaction, refers to the complex  
65 reactions between carbonyl-containing compound (such as reducing sugar) and amino-  
66 containing compound (such as amino acid, peptide or protein). It produces a complex array of  
67 compounds referred to as Maillard reaction products (MRPs) (Amarowicz, 2009). The rate of  
68 Maillard reaction (MR) is influenced by many factors, such as temperature, water activity  
69 ( $a_w$ ), pH, reactant source, concentration, type and ratio of reducing sugar to lysine, and time of  
70 exposure (Labuza & Baisier, 1992). The rate of deteriorative reactions and storage stability

71 are particularly linked to water activity of the non enzymatic browning reaction occurs at a  
72 maximal rate in the  $a_w$  range of 0.5–0.75 according to Kaanane & Labuza (1989) and Labuza  
73 & Saltmarch (1981). Among influencing parameters, temperature is considered as the main  
74 factor favoring the MR rate and strongly affecting the MRPs properties (Karseno, Yanto,  
75 Setyowati, & Haryanti, 2018; Zhang et al., 2018).

76 Furthermore, besides heating temperature, Jiang, Wang, Che, & Tian (2014) indicated that pH  
77 is an influencing factor, which modulates the MR rate, as they remarkably influence the  
78 biological activities and the characteristics of the MRPs. These include volatile compounds of  
79 low molecular mass, non-volatile colored compounds of intermediate molecular mass and  
80 brown melanoidins of high molecular weight exhibiting antioxidant properties (Loucif,  
81 Chetouani, Bounekhel & Elkolli, 2017; Lan et al., 2010). Previous studies demonstrated that  
82 MRPs might act as radical scavengers (Vhangani & Van Wyk, 2013), reducing agents  
83 (Loucif, Chetouani, Bounekhel & Elkolli, 2017) and metal chelators (Maillard, Billaud,  
84 Chow, Ordonaud, & Nicolas, 2007), based on their hydrogen atom and electron transfer  
85 capacity.

86 Recently, numerous scientific publications studied the effect of heating temperature on the  
87 functional properties of MRPs generated from coconut sap (Karseno, Yanto, Setyowati, &  
88 Haryanti, 2018), xylose and chicken peptide (Liu, Liu, He, Song, & Chen, 2015), galactose-  
89 bovine casein peptide (Jiang, Wang, Che & Tian, 2014), fructose–lysine and ribose–lysine  
90 model systems (Vhangani & Van Wyk, 2013) or silver carp protein hydrolysate–glucose  
91 system (You, Luo, Shen, & Song, 2011).

92 Additionally, heat-treatment of protein films and coatings or film forming protein solutions  
93 had a noticeable effect on film properties (Caoa, Fua, & Hea, 2007; Kim, Weller, Hanna, &  
94 Gennadios, 2002; Gennadios, Ghorpade, Weller, & Hanna, 1996). In this context, several  
95 studies showed that heat treatment improved the moisture barrier properties and the

96 mechanical toughness of cast films. It was observed for films made with soy protein  
97 (Gennadios, Ghorpade, Weller, & Hanna, 1996; Kim, Weller, Hanna, & Gennadios, 2002;  
98 Rhim, Gennadios, Handa, Weller, & Hanna, 2000), whey protein (Miller, Chiang, & Krochta,  
99 1997), collagen (Weadock, Olson, & Silver, 1984), zein, gelatin and fibrin proteins (Julius,  
100 1967). However, there is not enough information about the effect of heat treatment on the  
101 antioxidant activity of protein-based films.

102 In a previous study, we prepared a series of glucose-fish gelatin films and we promoted the  
103 MR by heating the films at 90 °C for 24 h. Resulted glucose-gelatin films displayed improved  
104 barrier, thermal and mechanical properties. In addition, these films exhibited an important  
105 antioxidant activity that was glucose/gelatin concentration and MR time dependent (Kchaou,  
106 et al., 2018). The present research aims to evaluate the effect of thermal treatments at  
107 different temperatures in the range of 90 to 130 °C and the impact of the Maillard reaction  
108 on the structure, and the functional and bioactive properties of gelatin based films with  
109 glucose or glucose free.

## 110 **2. Materials and methods**

### 111 *2.1. Materials*

112 Commercial fish gelatin type A (Rousselot 200 FG, 200 degree bloom, 4 mPa.s viscosity at  
113 45 °C for a concentration of 6.67% in water at pH = 5.4, water content of 11.77 g<sub>water</sub>/100g<sub>dry</sub>  
114 matter, ash content 0.10 g<sub>ash</sub>/100 g<sub>dry matter</sub>) was employed as filmogenic biopolymer for films  
115 preparation. Anhydrous glycerol was purchased from Fluka (98% purity, Fluka Chemical,  
116 Germany) and was used as plasticizer for the films. D(+) anhydrous-glucose (C<sub>6</sub>H<sub>12</sub>O<sub>6</sub>; 180  
117 g.mol<sup>-1</sup>) was used as reducing sugar to initiate the Maillard reaction in fish gelatin based  
118 films. All other reagents were of analytic grade.

### 119 *2.2. Film preparation*

120 A mother film-forming solution was prepared by dissolving fish gelatin 4% (w/v) in distilled  
121 water at 60 °C and was stirred for 30 min. The solution's pH was set fixed at 5.5 and was  
122 controlled during the following steps of film forming. Then, three different films were  
123 prepared from a mother film-forming solution. First of all, unplastized gelatin film named as  
124 (G) film was obtained by casting a volume of 25 ml of mother film forming solution in Petri  
125 dishes, drying in a ventilated climatic chamber (KBF 240 Binder, ODIL, France) at 25 °C and  
126 50% relative humidity (RH) for 24 h. Then, films were peeled from the surface. A plasticized  
127 gelatin film named (GP) film was prepared by adding glycerol to the mother film-forming  
128 solution at a concentration of 15% (w/w dry gelatin matter) and was stirred for 30 min. After,  
129 the same volume of the plasticized solution was poured and dried in the same conditions  
130 stated previously. Finally, plasticized glucose containing film, referred as (GP-glu) film was  
131 prepared to favour Maillard reactions development. For this, glucose was added to the  
132 plasticized film-forming solution at a 0.5/1.0 glucose/lysine molar ratio according to a  
133 previous study (Kchaou, et al., 2018). The same volume of the plasticized solution was  
134 poured and dried in same conditions described previously.

135 All prepared films were then equilibrated at 25 °C and 50% RH before the heating  
136 treatment and before all the analyses. Except for FTIR, XRD, TGA and DSC measurements,  
137 films were equilibrated at 0% RH.

138

### 139 *2.3. Heating treatments of films*

140 After peeling and equilibration, half of all the films (with or without glucose, plasticized and  
141 unplastized) were heated in an oven at 90, 100, 110, 120 and 130 °C for 24 h to induce  
142 Maillard reactions. Non heated films will be considered as blank and named as NH-G (non  
143 heated, unplastized films), NH-GP (non heated glycerol plasticized films) and NH-GP-glu  
144 (non heated glucose-glycerol plasticized films).

145 As the Maillard reaction is water activity dependent, the water activity of the sample prior  
146 heating was 0.5, corresponding to a water content lower than 7%. During the heating  
147 treatment, the water activity of films is rapidly equilibrated with the relative humidity in the  
148 oven, which ranges from 0.04 down to <0.01 when temperature rises from 90 to 130 °C  
149 (calculated from the room relative humidity introduced in the oven and the temperature in  
150 oven according the moist air thermodynamics (Mollier's diagram). Thus, the range of aw used  
151 is much below that of the maximum rate (Kaanane & Labuza, 1989; Labuza & Saltmarch,  
152 1981).

153

#### 154 *2.4. Film thickness*

155 Film thickness was measured using a digital thickness gauge (PosiTector 6000, DeFelsko  
156 Corporation, USA) with a one µm accuracy. For each film sample, five measurements at  
157 different positions were done.

#### 158 *2.5. Determination of the relative degree of crosslinking*

159 The relative degree of crosslinking was adapted from the method of Bubnis & Ofner (1992)  
160 and Prasertsung, Mongkolnavin, Kanokpanont & Damrongsakkul (2010). The concept of this  
161 method was to react free amino groups of gelatin, which indicate non-crosslinked groups,  
162 with 2,4,6-trinitrobenzene sulfonic acid (TNBS). This method only allows to measure the  
163 increase or decrease of the NH<sub>2</sub> groups related to an initial (un-heated films) NH<sub>2</sub> content. A  
164 negative relative crosslinking degree results from a hydrolysis of the peptide bonds within the  
165 protein as there are more terminal NH<sub>2</sub> groups. Approximately 10 mg of each gelatin film  
166 were weighed and placed into a test tube. Then, 1 mL of 0.01% TNBS solution and 1 mL of  
167 4% sodium hydrogen carbonate solution (NaHCO<sub>3</sub>, pH 8.5) were added. The reaction mixture  
168 was then heated at 40 °C for 2 h. At this step, the non-crosslinked primary amino groups of

169 gelatin react with TNBS and form a yellow soluble complex. This solution was further treated  
170 with 2 mL of 6 N HCl at 60 °C for 1.5 h in order to hydrolyze and dissolve any insoluble  
171 material. The absorbance of the solutions was determined spectrophotometrically at 415 nm.  
172 The measured absorbance of a sample was corrected with that of a blank tube prepared in the  
173 same manner except the reacted reagent (TNBS). The relative degree of crosslinking was then  
174 obtained from the difference between the absorbance values before and after crosslinking  
175 using the following equation (1):

$$\begin{aligned} 176 \quad & \text{Relative degree of crosslinking (\%)} \\ 177 \quad & = \left( 1 - \frac{\text{absorbance of crosslinked films}}{\text{absorbance of control films non heated}} \right) \times 100 \quad (1) \end{aligned}$$

178 Where NH-G film at 25 °C is the control film for G heated films, NH-GP film at 25 °C is the  
179 control film for GP heated films and NH-GP-glu film at 25 °C is the control one for GP-glu  
180 heated films.

## 181 2.6. Spectroscopic analysis

182 FTIR spectra of film samples were recorded with a Perkin-Elmer spectrometer (Spectrum 65,  
183 France) equipped with an attenuated total reflectance (ATR) accessory with a ZnSe crystal. 32  
184 scans were collected at a resolution of 2 cm<sup>-1</sup> in the wavelength range of 600-4000 cm<sup>-1</sup>.  
185 Calibration was performed using background spectrum recorded from the clean and empty  
186 cell at 25 °C. The Spectrum Suite ES software (Perkin Elmer) was used for FTIR data  
187 treatment.

188 The films were cut into rectangles (1 cm x 3 cm) and directly placed in the test cell of a UV-  
189 Visible spectrophotometer (SAFAS UVmc). Light transmission of the films was determined  
190 in the wavelength range from 200 to 800 nm according to the method used by Benbettaïeb,  
191 Karbowiak, Bornaz & Debeaufort (2015). An empty test cell was used as a reference.

192 2.7. Color properties

193 A CIE colorimeter (CR-200; Minolta, Japan) was used in order to assess the color changes in  
194 gelatin films as a function of heating temperature. A white standard color plate ( $L_0 = 97.5$ ,  $a_0$   
195  $= -0.1$ , and  $b_0 = 2.3$ ) was used as background for the color measurements of the films. Color  
196 of films was expressed as L (lightness/brightness), a (redness/greenness) and b  
197 (yellowness/blueness) values. The difference in color ( $\Delta E$ ) for GP-glu and GP films as a  
198 function of heating temperature was determined as follows:

199 
$$\Delta E = \sqrt{(L - L_c)^2 + (a - a_c)^2 + (b - b_c)^2} \quad (2)$$

200 L, a and b are the color parameters of the heated (GP and GP-glu) films;  $L_c$ ,  $a_c$  and  $b_c$  are the  
201 color parameters of their respective controls (non heated without glucose (NH-GP) and with  
202 glucose (NH-GP-glu) films). Three measurements were carried out for each sample and their  
203 average was obtained.

204 The obtained CIE Lab values were then used to calculate the browning index (BI) as  
205 mentioned in equation (3):

206 
$$BI = \frac{100(z - 0.31)}{0.172} \quad \text{with} \quad z = \frac{a + 1.75(L)}{5.645(L) + a - 3.012(b)} \quad (3)$$

207 2.8. Thermal properties

208 A thermogravimetric analysis (TGA) was carried out to determine the thermal stability of the  
209 film samples. This technique is based on the continuous weighing of the film as a function of  
210 the temperature rise in a controlled atmosphere (nitrogen). A TGA instrument (SDT Q 600)  
211 was used in order to assess the thermogravimetric measurements by heating the samples from  
212 25 to 600 °C at a heating rate of 5 °C/min under nitrogen atmosphere.

213 Thermal properties of films were investigated using a Differential Scanning Calorimeter  
214 (Mettler Instruments). About 5 mg of each film, initially weighed in sealed aluminium pans,  
215 were subjected to a double heating cooling cycle from -50 °C to 150 °C at a rate of 10  
216 °C/min, under nitrogen flow rate of 25 mL/min. Glass transition temperature (T<sub>g</sub>) for each  
217 sample was then determined from the mid-point of the second heating cycle using STAR<sup>e</sup>  
218 SW13.00 software (Mettler-Toledo DSC1). The C<sub>p</sub> variation (ΔC<sub>p</sub>) was also determined as an  
219 indicator of the film crystallinity variation after the heating treatment. Films were previously  
220 equilibrated at 25 °C and 0% RH during two weeks before each measurement to obtain the  
221 most dehydrated films for both of TGA and DSC analyses. Only two films were triplicated in  
222 order to determine the relative error measurement and thus a confidence interval of 10% was  
223 chosen for statistical analysis.

#### 224 2.9. X-ray diffraction (XRD) analysis

225 X-ray diffraction analysis of the selected films was performed using a diffractometer (D5000,  
226 Bruker) equipped with monochromatic Cu-Kα radiation (λ = 1.5418 Å) operating at a voltage  
227 of 40 kV and a current of 40 mA. All samples were analyzed in continuous scan mode with  
228 the 2θ ranging from 3° to 50° where θ is the incidence angle of the X-ray beam on the sample.

#### 229 2.10. Water content (WC) and water solubility (WS)

230 After being equilibrated at 50% and 25 °C, the water content (g<sub>moisture</sub>/100 g<sub>film</sub>) of gelatin  
231 films was determined by measuring the weight loss of samples (100 mg) after drying in an  
232 oven at 105 °C until constant weight was reached (dry sample weight) according to the  
233 following equation:

$$234 \quad WC = \frac{(m_0 - m'_f)}{m_0} \times 100 \quad (4)$$

235 where  $m_0$  is the initial film weight (g) and  $m'_f$  is the final film dry weight (g). Three samples  
236 of each formulation were analyzed.

237

238 The solubility of film samples in water was determined according to the Gennadios, Handa,  
239 Froning, Weller, & Hanna (1998) method. The film samples (2 cm x 5 cm) previously  
240 equilibrated were weighed and transferred to centrifuge tube containing 30 mL of distilled  
241 water with 0.1% (w/v) sodium azide as antimicrobial agent. The samples were then shaken at  
242 a speed of 250 rpm for 24 h at 25 °C. After centrifugation (GYROZEN centrifuge, 1580R) at  
243 8000 rpm for 10 min, samples were dried at 105 °C for 24 h and then were weighed to  
244 determine the remaining pieces of films. Water solubility (WS) was calculated as follows:

$$245 \quad WS(\%) = \frac{[(m_0 \times (100 - WC)) - m''_f]}{(m_0 \times (100 - WC))} \times 100 \quad (5)$$

246

247 where  $m_0$  : film initial weight (g) and  $m''_f$  : final dry weight of non-solubilised film (g). All  
248 tests were carried out in triplicate.

### 249 *2.11. Water contact angle*

250 The contact angle measurements were carried out using the sessile drop method on a  
251 goniometer (Drop Shape Analyzer 30 from Kruss GmbH), equipped with an image analysis  
252 software (ADVANCE). First, a droplet of water (~2 µL) was deposited on the film surface  
253 with a precision syringe. The method is based on image processing and curve fitting for  
254 contact angle measurement from a theoretical meridian drop profile, determining contact  
255 angle between the baseline of the water drop and the tangent at the drop boundary. Then, the  
256 contact angle was measured on both sides of the drop and averaged. Five measurements per

257 film were carried out. All the tests were conducted in an environmental chamber with a  
258 constant environment at a temperature of  $25\pm 2$  °C and a relative humidity of  $50\pm 1$ %.

## 259 2.12. *In-vitro* antioxidant activity

### 260 2.12.1. Free radical-scavenging activity (FRSA)

261 Two methods for assessing the free radical scavenging were used.

262

263 The antioxidant activity of films was first measured using the method of DPPH (2,2-diphenyl-  
264 1-picrylhydrazyl) free radical scavenging as described by Jridi et al. (2014), adapted to edible  
265 films. The films were cut into small pieces ( $m = 10$  mg) and immersed in 500  $\mu$ L of distilled  
266 water, 375  $\mu$ L of 99.5% ethanol and 125  $\mu$ L of 0.02% DPPH• in ethanol 99%. The mixtures  
267 were then incubated for 24 h at room temperature in the dark. The reduction of DPPH• radical  
268 was measured at 517 nm, using a UV–visible spectrophotometer. The DPPH• RSA was  
269 calculated as follows (equation 6):

$$270 \quad \text{DPPH radical scavenging activity}(\%) = \frac{A_c - (A_s - A_b)}{A_c} \times 100 \quad (6)$$

271 Where  $A_c$  is the absorbance of DPPH• solution without addition of the films,  $A_s$  is the  
272 absorbance of DPPH• solution containing the film samples and  $A_b$  is the absorbance of blank  
273 tubes containing film samples without addition of the DPPH• solution.

274 A lower absorbance of the reaction mixture, caused by the change of solution color from  
275 purple to yellow, indicated a higher radical-scavenging activity. The test was carried out in  
276 triplicate.

277

278 Antioxidant activity of films was also determined by the ABTS method as described by Re et  
279 al. (1999). The ABTS<sup>+</sup> radical was generated by mixing of 7 mM ABTS<sup>+</sup> stock solution and  
280 2.45 mM potassium persulphate ( $K_2S_8O_2$ ). Then, the mixture was placed under dark

281 conditions for 12-16 h before use. The ABTS<sup>+</sup> solution (stable for 2 days) was diluted with  
282 99.5% ethanol to adjust the absorbance to  $0.70 \pm 0.05$  at 734 nm. The films were cut into  
283 small pieces ( $m = 10$  mg) and immersed in 100  $\mu$ L of distilled water and 900  $\mu$ L of diluted  
284 ABTS<sup>+</sup> solution. The solution with samples was then incubated at 37 °C shielded from the  
285 light for 10 min, and a solution without samples under the same conditions was recorded as  
286 control. The absorbance was determined at 734 nm. The ABTS<sup>+</sup> radical scavenging activity  
287 could be expressed as follows:

$$288 \quad \text{ABTS}^+ \text{ radical scavenging activity (\%)} = \frac{A'_c - (A'_s - A'_b)}{A'_c} \times 100 \quad (7)$$

289 Where  $A'_c$  was the absorbance of the control ABTS<sup>+</sup> solution,  $A'_s$  was the absorbance of  
290 sample with ABTS<sup>+</sup> solution and  $A'_b$  was the absorbance of blank tubes containing film  
291 sample without the addition of ABTS<sup>+</sup> solution. The experiments were carried out in  
292 triplicate.

### 293 2.12.2. Reducing power

294 The ability of films to reduce iron (III) was determined according to the method of Yıldırım,  
295 Mavi & Kara (2001). Films were cut into small pieces ( $m = 10$  mg) and immersed in 0.5 mL  
296 of distilled water, 1.25 mL of 0.2 M phosphate buffer (pH 6.6) and 1.25 mL of 1% (w/v)  
297 potassium ferricyanide. After incubation for 3 h at 50 °C, a volume of 500  $\mu$ L of 10% (w/v)  
298 trichloroacetic acid was added to the mixture which was centrifuged for 10 min at 10,000  $\times g$ .  
299 Then, 1.25 mL of the supernatant solution of each sample mixture was mixed with 1.25 mL of  
300 distilled water and 0.25 mL of 0.1% (w/v) ferric chloride. After a reaction time of 10 min, the  
301 absorbance of the resulting solutions was measured at 700 nm. Higher absorbance of the  
302 reaction mixture indicated higher reducing power. The values are presented as the means of  
303 triplicate analyses.

304 2.12.3. *β-carotene-linoleate bleaching assay*

305 The ability of films to prevent β-carotene bleaching was determined according to the method  
306 of Koleva, Van Beek, Linssen, de Groot, & Evstatieva (2002). 0.5 mg β-carotene in 1 mL  
307 chloroform was mixed with 25 μL of linoleic acid and 200 μL of Tween-80. The chloroform  
308 was completely evaporated under vacuum in a rotator evaporator at 40 °C, then 100 mL of  
309 double distilled water were added, and the resulting mixture was vigorously stirred. The  
310 emulsion obtained was freshly prepared before each experiment. Aliquots (2.5 mL) of the β-  
311 carotene-linoleic acid emulsion were transferred to test tubes containing 10 mg of each film  
312 and 0.5 mL of distilled water. The tubes were immediately placed in water bath and incubated  
313 at 50 °C for 2 h. Thereafter, the absorbance of each sample was measured at 470 nm. Control  
314 tube was prepared in the same conditions without film. The antioxidant activity was evaluated  
315 in terms of β-carotene bleaching inhibition using the following formula:

316 
$$\beta - \text{carotene bleaching inhibition (\%)} = \left( 1 - \left( \frac{A_{\text{sample}}^0 - A_{\text{sample}}^{120}}{A_{\text{control}}^0 - A_{\text{control}}^{120}} \right) \right) \times 100 \quad (8)$$

317 where  $A^0$ : absorbance at  $t=0$  min,  $A^{120}$ : absorbance at  $t=120$  min.

318 2.12.4. *Inhibition of linoleic acid oxidation*

319 The lipid peroxidation inhibition activity of prepared films was measured in a linoleic acid  
320 emulsion system according to the method of Osawa & Namiki (1985). Film samples (10 mg)  
321 were added to 2.5 mL of phosphate buffer (50 mM; pH 7.0), 2.5 mL of absolute ethanol and  
322 0.0325 mL of linoleic acid. The final volume was then been adjusted to 6.25 mL with distilled  
323 water. The reaction mixture was incubated in glass test tubes with aluminum screw caps at 45  
324 °C for 10 days in a dark room. A tube without sample addition was used as negative control.  
325 The degree of linoleic acid oxidation during time storage was measured by the evaluation of

326 the thiobarbituric acid reactive substances (TBARS) formation, including malondialdehyde  
327 (MDA). TBARS were assayed, every three days, by the method described by Yagi (1976).  
328 MDA and TBARS were measured by their reactivity with TBA in an acidic condition to  
329 generate pink colored chromospheres, which absorb at 530 nm. The capacity of the TBARS  
330 formation inhibition in linoleic acid system was determined as follows:

$$331 \quad \text{Lipid peroxidation inhibition capacity (\%)} = 1 - \left( \frac{A_{\text{Sample}}}{A_{\text{Control}}} \right) \times 100 \quad (9)$$

332 Where  $A_{\text{sample}}$  is the absorbance value of the film sample and  $A_{\text{control}}$  is that of the pure linoleic  
333 acid used as the standard.

### 334 2.13. Activation energy

335 The Arrhenius model was used to calculate the activation energy ( $E_a$ ) for  $\Delta E$ , BI,  
336  $A_{294\text{nm}}$ ,  $A_{420\text{nm}}$ , water solubility, relative crosslinking degree, free radicals (DPPH• and  
337 ABTS<sup>+</sup>) scavenging activity,  $\beta$ -carotene-linoleate bleaching assay as well as reducing power  
338 parameters. The  $E_a$  was determined from the value at equilibrium, and not from the kinetic  
339 rates on each parameter.  $E_a$  allows to determine the dependence of the MR on the heating  
340 temperature on all the studied parameters. The activation energy was deduced from the  
341 following mathematical Arrhenius-equation established by Vant'Hoff in 1884, which was well  
342 described in the literature (Labuza, 1984):

$$343 \quad \ln(x) = f\left(\frac{1}{RT}\right) \quad (10)$$

344 where  $\ln(x)$  corresponds to the natural logarithmic (Ln) of the studied variable ( $x$ ),  $R$  is the  
345 universal gas constant (8.314 J/mol K) and  $T$  is the absolute temperature (K). Then,  $E_a$  was  
346 obtained by calculating the slope of the linear part of the plot of the logarithm of ( $x$ ) vs ( $1/$   
347  $RT$ ). When only a part of the plot displayed a significant linear behavior, the  $E_a$  was  
348 calculated on a limited range of temperature and was specified. Furthermore, the linear

349 regressions ( $R^2$ ) of the corrected experimental fitting points of the Arrhenius plots were  
350 determined.

#### 351 *2.14. Statistical analysis*

352 Statistical analyses were performed with SPSS ver. 17.0, professional edition using ANOVA  
353 analysis at a (p-value<0.05). Duncan's multiple-range test (p-value<0.05) was used to detect  
354 differences among mean values of all the parameters analyzed for the different films. A  
355 standard deviation at the 90% confidence level was used to compare the DSC data for the  
356 different films.

### 357 **3. Results and discussion**

#### 358 *3.1. Confirmation of the crosslinking in fish gelatin films induced by temperature and/or* 359 *Maillard reaction*

360 The relative degree of crosslinking, FTIR, color change and UV absorption were  
361 techniques selected to assess the efficacy of the thermal treatment and Maillard reaction to  
362 induce crosslinking but also to generate new compounds able to have positive effect on the  
363 functional properties of films.

##### 364 *3.1.1. The relative crosslinking degree*

365 The relative crosslinking of films heated at different temperatures has been evaluated  
366 by measuring the loss of free amino groups using the TNBS method. Even if the TNBS  
367 method is an indirect method of assessing the crosslinking, it allowed to display the change in  
368 the number of free amine groups, and thus the indirect evaluation of the amine function  
369 engaged in crosslinking. Crosslinking degree is a relative value regarding the number of free  
370 amino groups at 25 °C, *ie* determined on non-heated films. The negative value of the relative  
371 crosslinking degree of the unplasticized glucose-free gelatin (G) films is explained by the

372 hydrolysis of the gelatin chains with high temperature, which is mainly involved for  
373 temperatures higher than 100 °C (Fig. 1).

374 For GP-glu films, the relative crosslinking degree increased significantly from 33.6%  
375 to 55.5% with increasing the temperature from 90 to 130 °C, respectively. This confirms the  
376 consumption of a fraction of the free amino acids during the protein-glucose conjugation.  
377 Results showed that the variation of relative crosslinking degree follows a linear trend as a  
378 function of heating temperature. Nevertheless, only 55.5% of crosslinking has been revealed  
379 at the highest temperature indicating that 44.5% of the amino groups were still in the free  
380 form and available for further reactions, linked to the free amino groups available at 25 °C  
381 (non-heated films). You, Luo, Shen, & Song (2011) reported that the temperature plays an  
382 important role on the ultimate content of free amino acids, which determines the formation  
383 rate of MRPs. Loucif, Chetouani, Bounekhel & Elkolli (2017) stated that the crosslinking  
384 degree increased to about 45%, 47% and 56% for alginate/gelatin crosslinked systems  
385 prepared at pH 11 and heated at 70, 80 to 90 °C, respectively. Jiang, Wang, Che & Tian  
386 (2014) displayed a continuous decrease of the free amino groups in galactose-bovine casein  
387 peptide systems upon heating ranging from 70 to 120 °C which achieved 51.1% after heat  
388 treatment at 120 °C. The increase in relative crosslinking values (%) is correlated with the  
389 increase in the browning intensity values (Table 1) in gelatin-glucose films confirming that  
390 the heating temperature range used was effective for promoting the MR. For glucose-free  
391 gelatin films, the relative crosslinking degree, caused only by the thermal treatment, was  
392 13.6%, 17.2%, 25.5%, 26.3% and 28.5% for 90, 100, 110, 120 and 130 °C, respectively. Such  
393 findings showed that the thermal treatment in absence of glucose facilitate also possible  
394 reactions/interactions between amino acid residues of gelatin, including inter-protein and  
395 intra-protein crosslinking. Glycerol is present in the glucose-free gelatin films and can  
396 promote MR as it plays as a precursor. This was demonstrated by Smarrito-Menzozi,

397 Matthey-Dorret, Devaud-Goumoens & Viton (2013) and Cerny & Guntz-Dubini (2006). The  
398 browning and crosslinking that occurred in glucose-free gelatin films could then be explained  
399 by the glycerol effect.

400 The activation energies of crosslinking degree are respectively 23.3 and 16.1 kJ/mol for GP  
401 and GP-glu films. Glucose thus makes the crosslinking easier as it requires less energy. This  
402 is logical as crosslinking results of MR were enhanced by the glucose.

### 403 *3.1.2. FTIR spectroscopy*

404 The ATR-FTIR spectroscopy was used in this study in order to assess the chemical  
405 bond modifications following the establishment of interactions in glucose-free gelatin as well  
406 as in gelatin-glucose films after heating treatments. Results presented in Fig. 2 showed that  
407 similar spectra were obtained for both films. As it can be seen, gelatin films displayed three  
408 characteristic peaks located at 1642-1654  $\text{cm}^{-1}$ , 1540-1551  $\text{cm}^{-1}$  and 1239-1243  $\text{cm}^{-1}$  related to  
409 C=C and C=O stretching of primary and secondary amine N-H band of amide-I, N-H bending  
410 of amide-II and assigned to aromatic primary amine and C-N and N-H stretch of amide-III or  
411 vibrations of  $\text{CH}_2$  groups of glycine, respectively (Hoque, Benjakul, & Prodpran, 2011).  
412 Loucif, Chetouani, Bounekhel & Elkolli (2017) reported a similar spectrum for gelatin films  
413 where the amide-I, amide-II and amide-III peaks were located at 1646, 1550 and 1237  $\text{cm}^{-1}$ ,  
414 respectively. Additionally, a peak situated around 1046  $\text{cm}^{-1}$  is present in the different films  
415 spectra. This peak might be related to the possible interactions arising between the plasticizer  
416 (OH group of glycerol) and gelatin (Bergo & Sobral, 2007). Furthermore, small shifts in  
417 amide-I, amide-II and amide-III positions have been noted for GP-glu films when heating  
418 temperature increased up to 130 °C. In fact, the latter bands shifted from 1648  $\text{cm}^{-1}$  to 1646  
419  $\text{cm}^{-1}$ , from 1551  $\text{cm}^{-1}$  to 1545  $\text{cm}^{-1}$  and from 1243  $\text{cm}^{-1}$  to 1240  $\text{cm}^{-1}$  for amide I, amide II and  
420 amide III peaks, respectively for 130 °C heated glucose-gelatin films. Etxabide, Urdanpilleta,  
421 Gómez-Arriaran, de la Caba, & Guerrero (2017) reported that the changes in the secondary

422 structure of fish gelatin-lactose films prepared at native pH (5.4) and heated at 105 °C for 24 h  
423 were not so noticeable and the chain movement was restricted. In the present study, the 130  
424 °C heated glucose-free gelatin films display amide I and amide II bands shifted from 1654  
425  $\text{cm}^{-1}$  to 1647  $\text{cm}^{-1}$  and from 1551  $\text{cm}^{-1}$  to 1546  $\text{cm}^{-1}$ , respectively. However, no modification  
426 in the amide III position has been revealed for control films. In the end, the FTIR only reveals  
427 weak changes in the chemical structure of gelatin network, either because no new type of  
428 bonds occurred, or new linkage are of similar nature as those already existing in the gelatin, or  
429 new linkage are in too low proportion to be clearly displayed.

### 430 *3.1.3. Color of films*

431         Optical properties are essential to define the ability of films to be applied over a food  
432 surface, due to their effect on the appearance of coated foods (Abdelhedi et al., 2018).  
433 Changes in color of glucose-free gelatin and gelatin-glucose films as a function of heating  
434 temperature were determined and shown in table 1. As can be seen, a considerable decrease in  
435 L-values of gelatin-glucose films was observed with increasing temperatures up to 110 °C. As  
436 the L-value is related to the lightness of a sample, it reflected the development of dark  
437 products after 24 h of heating due to MR. In addition, heating gelatin-glucose films at high  
438 temperatures led to increase significantly their dark-yellowish color as illustrated in Fig. 3 and  
439 as proved by b-values measurements. Indeed, b-values first increased rapidly when  
440 temperature rose from 90 to 110 °C, and then its rate increased slowly in the temperature  
441 range between 110 and 130 °C.

442 However, the b-values of GP films showed a slight increase until 120 °C and then increased  
443 remarkably at 130 °C to reach a value of 7.8. It reveals the beginning of a yellowish color  
444 appearance (Fig. 3). In this context, Leceta, Guerrero, & de la Caba (2013a) reported that  
445 color parameters changed notably for chitosan-based films after being heat-treated at 105 °C  
446 for 24 h, which could mean that the film structure changed. Furthermore, total color

447 difference ( $\Delta E$ ) was measured in order to assess the observed differences between heated  
448 films and their non-heated films. A sharp increase in  $\Delta E$ -values was noticed as a function of  
449 heating temperature for GP-glu films up to 110 °C. Such results of  $\Delta E$ -values indicated that  
450 MR resulted films are dark colored and their barrier ability in the visible region is stronger  
451 than that of non heated gelatin films (Fig. 4).  $\Delta E$ -values for GP films require 5 times more  
452 energy when the  $E_a$  rises from 25 to 122.1 kJ/mol (table 3, supplementary data). Furthermore,  
453 the browning index (BI), was calculated for GP-glu films and displayed a similar trend to  $\Delta E$   
454 and b-values. The browning index give an overall evaluation of the progress of the Maillard  
455 reaction according the development of colored compounds generated. It increased  
456 significantly with heating temperatures, from  $22.44 \pm 1.10$  at 90 °C to  $85.35 \pm 6.93$  at 130 °C.

#### 457 *3.1.4. UV-visible spectroscopy*

458 In order to correlate the visual variation of film's color with the elaboration of MRPs,  
459 the UV-visible light absorbance of glucose-free gelatin (GP) and gelatin-glucose (GP-glu)  
460 films was conducted in the range of 200–800 nm and spectra are presented in Fig. 4. All  
461 prepared gelatin films displayed an excellent UV light barrier capacity in the range of 200 nm  
462 to 300 nm due to the presence of aromatic amino acids namely tyrosine and phenylalanine that  
463 absorb UV light (Li, Liu, Gao, & Chen, 2004). For heat-treated glucose-free gelatin films, a  
464 slight increase of the UV-absorption (250-350 nm) as a function of the temperature (until 120  
465 °C) has been revealed that thermal treatment was not the main factor affecting the UV-light  
466 barrier properties of gelatin films. However, the absorbance increases noticeably in the range  
467 of 250-400 nm for 130 °C heat-treated films. Regarding GP-glu films, they displayed  
468 different spectra ranging from 200 nm to 500 nm. Their absorbances increased markedly of  
469 about 6 times until 120 °C to be mainly constant at 130 °C. These results are in line with the  
470 color data because these films are also lightly colored. The concomitant rise of absorption

471 indicated the development of MRPs. Therefore, all the GP-glu heat-treated films and the 130  
472 °C heated GP films effectively prevented UV light. Their potential preventive effects on the  
473 retardation of product oxidation induced by UV light is expected (Leceta, Guerrero, & de la  
474 Caba, 2013a).

475           After the first step of MR, which consists on the condensation reaction between the  
476 carbonyl group of glucose and the amino group of gelatin, unstable products known as Schiff  
477 base products are formed and then transformed via the Amadori rearrangement into protein-  
478 bound Amadori products (Etxabide, Urdanpilleta, Gómez-Arriaran, de la Caba, & Guerrero,  
479 2017). These latter are intermediate colorless compounds absorbing in the UV-light (294 nm).  
480 Fig. 5.A indicated that the absorbance at 294 nm ( $A_{294\text{nm}}$ ) of GP-glu films was significantly  
481 higher than that of GP films for the different heating temperatures, except for non-heated  
482 films. As can be seen, glucose-free gelatin films didn't show any variation of  $A_{294\text{nm}}$  values up  
483 to 120 °C. However, an increase in absorbance values has been noted for 130 °C heated  
484 gelatin films. For gelatin-glucose (GP-glu) films,  $A_{294\text{nm}}$  values increased markedly when MR  
485 heating temperature increased from 90 to 110 °C and then reached a plateau at 110 °C. This  
486 finding could be due to the transformation (at temperatures higher than 110 °C) of the  
487 intermediate compounds into the final MRP's during the further steps of the Maillard  
488 reaction. This was showed by the higher absorbance at 420 nm thanks to MRPs. Indeed,  
489 Arrhenius representations (supplementary data) clearly display the change in activation  
490 energy below and above 120 °C and the  $E_a$  rose respectively from 24.1 to 133.8 kJ/mol for  
491 the glucose-free gelatin (GP) films. You, Luo, Shen, & Song (2011) reported that  $A_{294\text{nm}}$   
492 values obtained for silver carp protein hydrolysate-glucose system at the temperature of 60°C  
493 were significantly higher than those obtained at 50 °C.

494           Further progress of the MR involves the production of high molecular weight  
495 compounds, termed melanoidins, with chromophore groups having a characteristic

496 absorbance at 420 nm (Delgado-Andrade, Seiquer, Haro, Castellano, & Navarro, 2010).  
497 Indeed, the 420 nm absorbance is directly related to the presence of cycle structures, typical of  
498 melanoidins and Amadori rearrangement resulting compounds. These brown nitrogenous  
499 compounds have been frequently used to evaluate the extent of this reaction (Nasrollahzadeh,  
500 Varidi, Koocheki, & Hadizadeh, 2017). Fig. 5.B illustrated the absorbance at 420 nm of GP  
501 and GP-glu films as a function of heating temperature. The absorbance at 420 nm was  
502 significantly different between GP and GP-glu films at all temperatures except at 25 °C. GP  
503 films didn't show a specific absorbance at 420 nm regardless increasing heating temperature  
504 up to 120 °C ( $A_{420} \approx 0.06$ ). Nevertheless, heating at 130 °C increased notably the absorbance  
505 ( $A_{420} = 0.192$ ) of glucose-free gelatin (GP) films as previously observed for absorbance at 294  
506 nm. For GP-glu films, a high increase in  $A_{420}$  values has been noted which was linearly  
507 heating temperature-dependent. These findings showed that the brown yellowish color  
508 development because of the Maillard reaction was extremely dependent on temperature and  
509 thus, the formation of colored melanoidins was faster at higher heating temperatures. This is  
510 in accordance with previously obtained BI results. In this context, Lan et al. (2010) reported  
511 similar results in terms of  $A_{420}$  values for both xylose–soybean peptide MRPs and thermal  
512 degradation products, prepared at temperatures ranging from 80°C to 130 °C. The authors  
513 indicated that browning development was almost completely due to the MR in the soybean  
514 peptides–xylose system and slightly influenced by thermal degradation and sugar  
515 caramelization. Jiang, Wang, Che & Tian (2014) reported a high correlation ( $R^2 = 0.913$ )  
516 between the heating temperature (70-120 °C) and the browning intensity ( $A_{420}$ ) of galactose-  
517 bovine casein peptide MRPs. Furthermore, Etxabide, Urdanpilleta, de la Caba, & Guerrero  
518 (2016) reported that the increase in the absorption above 420 nm for gelatin-lactose films  
519 prepared at native pH (5.4) and heated at 105 °C for 24 h, is due to the fact that the

520 crosslinking reaction reached the final stage, in which melanoidins, brown and non-soluble  
521 compounds, were formed.

522           Similar trends of variation as a function of heating temperature have been noted for b,  
523  $\Delta E$  and BI indicating the development of yellow-brown MRPs, caused by the melanoidins  
524 color. Furthermore, the  $E_a$  was higher in the case of GP films compared to GP-glu films in the  
525 case of  $A_{294nm}$  and  $A_{420nm}$  values (Table 3). All these characterizations confirm that MR  
526 occurs in GP-glu films, but probably also in the GP films, either due to glycerol (Smarrito-  
527 Menozzi, Matthey-Dorret, Devaud-Goumoens & Viton, 2013) or to sugar impurities in  
528 gelatin.

529

### 530 *3.2. How temperature and Maillard reactions changed the structure of gelatin-based films*

#### 531 *3.2.1. Thermal properties*

532           The thermal stability of gelatin films crosslinked or not with glucose and heated at  
533 temperatures ranging from 90 to 130 °C was assessed by means of TGA in a range of  
534 temperature between 25 and 600 °C. The weight loss ( $\Delta w$ ), temperature of maximum  
535 degradation ( $T_{max}$ ) and final residual mass (Residue %) of the different films are illustrated in  
536 table 2. The TGA curves (data not shown) of GP and GP-glu films indicated two steps of  
537 transformations corresponding to the main stages of weight loss. The first stage of  
538 transformation is related to the loss of free and bound water (below 100 °C). The weight loss  
539 in this step was ranged from 4% to 8%. The second stage of weight loss, corresponding to  $\Delta w$   
540 around 69% and 77%, displayed the degradation or the decomposition of gelatin chains at  
541 approximately 303-314 °C. Results presented in table 2 showed that MR increases the  $T_{max}$   
542 from 310 to 314 °C after 24 h of heating at 90 °C, whereas, there is no differences in  $T_{max}$   
543 values when MR temperature increased from 90 to 130 °C. For glucose-free gelatin (GP)

544 films, the thermal stability increased by heating at  $T \geq 120$  °C. Such thermal resistance rise in  
545 control films could be due the generation of new bonds or interactions between gelatin strings,  
546 which favored their thermal stability. Furthermore, the development of MRPs, which could  
547 interact with gelatin chains to stabilize the protein network, may explain the increase in the  
548 observed thermal stability for gelatin-glucose films heated at high temperatures (90-130 °C)  
549 (Kchaou et al., 2018, González Seligra, Medina Jaramillo, Famá & Goyanes, 2016).

550 The thermal properties of glucose-free gelatin (GP) and gelatin-glucose (GP-glu) and  
551 unplasticized gelatin (G) films were assessed by the DSC analysis in order to determine the  
552 glass transition temperature ( $T_g$ ) from the second heating cycle and the  $\Delta C_p$  (Table 2). As  
553 expected, the  $T_g$  value of the unplasticized films is much greater than that of GP and GP-glu  
554 films. Indeed, it is well known that adding glycerol in the film recipe induces a plasticization  
555 revealed by the  $T_g$  value decrease by 25 °C. Moreover, the addition of glucose, even at low  
556 ratio, also decreased the  $T_g$  value but to a smaller extent (non-significant). The plasticizing  
557 effect of glucose is less efficient than that of glycerol as demonstrated by Simperler et al.  
558 (2006).

559 All films displayed a clear increase in the  $T_g$  values with increasing the temperature of  
560 treatment. The increase of  $T_g$  values in hydrophilic biopolymer network could be due either to  
561 water content decrease, or to crosslinking/reticulation very often simply attributed as an  
562 antiplasticization phenomenon. In our case, the water content did not change significantly as  
563 all the films were previously equilibrated at 0% relative humidity. The rise of  $T_g$  value could  
564 thus be attributed to a crosslinking/reticulation. However, not only the Maillard reactions are  
565 responsible of the crosslinking as it occurs also in glucose-free films and in unplasticized  
566 films. Indeed, the  $T_g$  rose from 77 °C to 86 °C for unplasticized G films, from 51 °C to 65 °C  
567 for GP films and from 45 °C to 64 °C for GP-glu films when temperature range from 25 to  
568 130 °C, respectively.

569 Furthermore, the higher the  $\Delta C_p$ , the lower the crystallinity, as the  $\Delta C_p$  is only related to  
570 the amorphous phase. From table 2, the higher  $\Delta C_p$  is obtained for the unplasticized gelatin  
571 (G) films. Adding glycerol or glucose induced plasticization and thus chain mobility, which  
572 could make crystallization easier (chain rearrangement in a more ordered configuration). This  
573 is confirmed by the decrease of the  $\Delta C_p$  values for GP and GP-glu films. By comparing the  
574 effect of heat treatment, the  $\Delta C_p$  of the GP-glu films increased because of favoured  
575 crosslinking enhanced by the Maillard reaction, which limits chain mobility and thus  
576 recrystallization.

577 Moreover, it appears clearly that the improvement of thermal resistance of GP-glu films  
578 measured from TGA could be both due to the effects of MR and to a supposed crystallinity  
579 increase. Additionally, the increase in  $T_g$  values is in accordance with the increase in  
580 crosslinking degrees. In this context, Hoque, Benjakul & Prodpran (2010) reported that  
581 generally, the increased crystallinity, molecular weight, ionic degree and crosslinking increase  
582  $T_g$ .

### 583 3.2.2. X-ray diffraction (XRD)

584 Furthermore, the XRD analysis was carried out in order to assess the structural  
585 modifications and the molecular conformation changes caused by the thermal treatment and  
586 MR in prepared gelatin films (Fig. 6). The diffractograms of all the films showed a sharp peak  
587 at about  $8^\circ$  ( $2\theta$ ), and a broad peak at about  $20^\circ$  ( $2\theta$ ). The other sharp peaks could be attributed  
588 to the inorganic impurities (salts, metals) in the gelatin powder, in which the ash content  
589 corresponds to around 0,14% of dry matter. The sharp strong peak is due to the triple helix  
590 structure, whose peak position corresponds to the diameter of triple helix, and the intensity  
591 corresponds to the triple helix content. The broad amorphous peak located at  $20^\circ$  ( $2\theta$ ) is  
592 related to the distance between amino acid residues along the helix (Liu et al., 2016). Loucif,

593 Chetouani, Bounekhel & Elkolli (2017) reported similarly that the spectrum of gelatin film  
594 exhibited two peaks ascribed to helical crystalline structure of collagen renatured in gelatin,  
595 the first small and narrow peak is at  $2\theta = 7.75^\circ$  and the second broad one at  $2\theta = 20.08^\circ$ . A  
596 slight displacement of the first peak position ( $2\theta = 8^\circ$ ), has been noted for 90 °C GP films  
597 compared to NH-GP films. However, this peak disappears for 130 °C applied to GP films  
598 indicating a loss of the triple helix structure at 130 °C. For GP-glu films, there were no  
599 significant displacements of the sharp peak position as a function of heating temperature,  
600 indicating a constant triple helix diameter. For 130 °C, this peak tends to disappear for GP-glu  
601 films as previously observed for GP films. Regarding the triple helix content, it decreases  
602 remarkably as a function of heating temperature as evidenced by the decrease in the intensity  
603 of the sharp peak ( $8^\circ$ ) for GP films as well as for the GP-glu films. For the broad peak ( $2\theta =$   
604  $20^\circ$ ), its position increased up to 130°C with increasing heating temperature for GP films .  
605 Similar observations have been obtained for GP-glu films up to 90 °C. For 130 °C, this peak  
606 was almost absent in GP-glu films confirming the loss of the structure of triple helix. The  
607 structural and functional properties of proteins can be influenced by heat treatment leading to  
608 the proteins denaturation by the destruction of some forces that stabilize native conformations,  
609 such as hydrogen bonds, electrostatic, hydrophobic and disulfide bonds (Pirestani, Nasirpour,  
610 Keramat, Desobry -& Jasniewski, 2018). Additionally, Caoa, Fua, & Hea (2007) reported that  
611 heating denatures secondary and tertiary structures of proteins and allows possible disulfide  
612 interchanges among protein molecules.

613

### 614 *3.3. Film functional properties modified by temperature and Maillard reactions*

615 Water resistance properties including water content (WC), water solubility (WS) and  
616 water contact angle (WCA) of glucose-free gelatin and gelatin-glucose films were  
617 characterized and the results are showed in Fig. 7.

### 618 3.3.1. Water content

619 Water content didn't show a significant modification despite of increasing heating  
620 temperature values up to 120 °C for both GP and GP-glu films (Fig. 7.A). However, a  
621 significant decrease in WC values has been noted for 130 °C for all films. This finding is  
622 explained by the loss of free water from films heated at 130 °C.

### 623 3.3.2. Water solubility

624 For instance, partial water solubility in the saliva could be set for applications of  
625 edible films as coating. Water solubility (WS) was calculated based on the percentage of  
626 soluble matter to initial dry matter in each film sample (Kim, Weller, Hanna, & Gennadios,  
627 2002). WS of all films is shown in Fig. 7.B. Results highlighted that solubility values are kept  
628 invariable for G and GP films heated at 90 and 100 °C compared to non-heated films (NH-  
629 GP). However, heating at higher temperature ( $\geq 110$  °C) decreased remarkably the films  
630 solubility from 75% to 23%. The relative crosslinking degree values of G and GP films  
631 explain the solubility values. Indeed, the higher the crosslinking, the lower the solubility.

632 For GP-glu films, a high reduction in water solubility values has been obtained from  
633 24.33% to 13.85% for GP-glu films heated from 90 to 130 °C, respectively when the value  
634 was initially 69.26% for NH-GP-glu films. These results displayed that MR and heat  
635 treatment are effective methods for reducing the solubility of gelatin-based films. Heating  
636 temperature higher than 100 °C did not greatly influence the water solubility of GP-glu  
637 crosslinked films. Etxabide, Urdanpilleta, de la Caba, & Guerrero (2016) reported that lactose  
638 addition reduced significantly ( $p < 0.05$ ) the solubility of gelatin films prepared at native pH  
639 (5.4) and heated at 105 °C as a result of the higher extent of glycation due to the formation of  
640 non-soluble compounds, melanoidins. Reduction in water solubility following heat treatments  
641 has also been documented by Kim, Weller, Hanna, & Gennadios (2002) for soy protein films.

642 They suggested that covalent crosslinking, caused by heat denaturation of protein, is  
643 responsible for film water insolubility. Furthermore, since total color difference and water  
644 solubility followed the same trend of variation as a function of MR heating temperature, it can  
645 be concluded that the development of MRPs reduced significantly the water solubility of  
646 gelatin films. It has been largely reported in the literature that the early stage of the Maillard  
647 reaction involves the formation of conjugates between the carbonyl group of the carbohydrate  
648 ends with the amine group of proteins, producing a Schiff base. The Schiff base subsequently  
649 cyclizes to produce the Amadori compounds and then colored and insoluble polymeric  
650 compounds (referred to as melanoidins) are formed (Yasir, Sutton, Newberry, Antrews, &  
651 Gerardard, 2007; Leceta, Guerrero, & de la Caba, 2013a; Leceta, Guerrero, Ibarburu, Duenas,  
652 & de la Caba, 2013b; Duconseille, Astruc, Quintana, Meersman & Sante- Lhoutellier, 2015).

653 Additionally, results showed that the water solubility activation energy of GP-glu  
654 films was reduced indicating that the glucose addition made the enhancement of water  
655 sensitivity of films easier, especially in the range of 90-100 °C (as revealed by the Arrhenius  
656 plot given in the supplementary data). Indeed, the  $E_a$  decreased from -5.0kJ/mol to -59.8  
657 kJ/mol for glucose-free unplasticized gelatin (GP) films and glucose-gelatin (GP-glu) films,  
658 respectively.

659

### 660 *3.3.3. Water contact angle*

661 Furthermore, water contact angle (WCA) is a good indicator of the hydrophilicity  
662 degree of films. The final state of a water drop on the film surface is taken as an indication of  
663 surface wettability (Leceta, Guerrero, & de la Caba, 2013a). The surface properties of GP and  
664 GP-glu films were evaluated by WCA measurements (Fig. 7.C). Results showed that the  
665 water contact angle values of GP films didn't vary significantly up to a temperature of 120°C.

666 However, GP films heated at 130 °C display a significant WCA value decrease from 104° to  
667 77° indicating that heating temperature leads to an increase of gelatin films hydrophilicity.  
668 For the GP-glu films, only those heated at  $T \geq 110$  °C showed a significant decrease in WCA  
669 values compared to NH-GP-glu films. Leceta, Guerrero, Ibarburu, Duenas, & de la Caba.  
670 (2013b) reported that the heat-treatment caused a slight decrease in contact angle values,  
671 attributed to changes in the conformation of molecules and to the exposure of the hydrophilic  
672 groups toward the surface.

### 673 *3.4. Antioxidant activity*

674 The antioxidant activity of MRPs is complex. Thus, it is necessary to employ a  
675 number of antioxidant indices to obtain a holistic view of the antioxidant pattern or  
676 mechanisms of MRPs (Vhangani & Van Wyk, 2013). The antioxidant potential of GP and GP-  
677 glu films was assessed by the free radical scavenging activity (FRSA) using DPPH• and  
678 ABTS radicals, the reducing power (RP), the  $\beta$ -carotene bleaching inhibition and the linoleic  
679 acid oxidation inhibition assays.

#### 680 *3.4.1. DPPH• free radical scavenging activity (FRSA)*

681 The DPPH• scavenging activity of all the gelatin films (G, GP and GP-glu) heated at  
682 90, 100, 110, 120 and 130 °C is shown in Fig. 8.A. The G and GP (unplasticized and  
683 plasticized) films display the same behavior with the temperature changes. For these films, the  
684 rise of the FRSA only occurred at temperatures higher than 110 °C. The ability of GP-glu  
685 films to scavenge DPPH• free radicals is due to their hydrogen atom transfer capacity, which  
686 increased clearly after the MR. Indeed, this increase in FRSA was temperature dependent for  
687 GP-glu films up to 100 °C. Thereafter, a sharp decrease in FRSA was found when heating  
688 temperature increased from 110 °C to 130 °C which could be attributed to the conformational  
689 change and protein denaturation. These findings revealed that heating temperature is a crucial

690 factor for controlling MRPs formation where increasing temperature up to 100 °C was enough  
691 to enhance the antioxidant activity of GP-glu films. Also, with the enhanced crosslinking with  
692 temperature, the release of the active MRPs is probably limited. Indeed, the farther the Maillard  
693 reaction goes with the temperature, the bigger size the MRPs is. The greater the crosslinking  
694 and the size of polymerized MRPs is, the lesser the molecular mobility and thus probably  
695 lower the release of the active compounds in the DPPH• media is. In this context, Sun & Luo  
696 (2011) reported an increase of FRSA by 480% for porcine haemoglobin hydrolysate–sugar  
697 model system when MR temperature rose from 40 to 85 °C. Loucif, Chetouani, Bounekhel &  
698 Elkolli (2017) reported that there was a positive relationship between the antioxidant capacity  
699 and MRPs, particularly compounds crosslinked at higher temperature conditions. For GP  
700 films, different results were observed. GP films heated at 90 °C showed the same activity than  
701 that of NH-GP films which was equal to 33.88%. The DPPH• activity of NH-GP films, even  
702 it was low, could be related to the presence of some antioxidant peptides probably elaborated  
703 during the gelatin extraction process (Jridi et al., 2017). Nevertheless, increasing heating  
704 temperature from 100°C to 130 °C lead to a significant increase in the radical scavenging  
705 activity of GP films that reached around 91% at 130 °C. This could be due to the thermal  
706 degradation of gelatin at high temperatures, which generated small active peptides and thus  
707 enabling their release. Similarly, Yu et al. (2018) reported a significant increase ( $p < 0.05$ ) for  
708 DPPH• radical-scavenging activity of different peptide fractions of soybean meal hydrolysate  
709 by heating at 120 °C for 2 h. The authors indicated that the thermal degradation might  
710 occurred during the heating process and would lead to the changes in antioxidant activity.

#### 711 *3.4.2. ABTS<sup>+</sup> radical scavenging activity*

712 Furthermore, the ABTS<sup>+</sup> radical scavenging activity was used in order to assess the  
713 antioxidant potential of prepared films. As shown in Fig. 8.B, the activity of NH-GP films  
714 was similar to the GP films heated at 90 °C ( $\approx 38\%$ ). Ge et al. (2018) reported that films

715 exhibited a low ABTS<sup>+</sup> radical scavenging activity that is attributed to the electron donation  
716 ability of some amino acids of gelatin, which reduces ABTS<sup>+</sup> radicals to offer weak  
717 antioxidant activity. However, increasing heating temperature ( $T \geq 100$  °C) leads to a slight  
718 increase of the ABTS<sup>+</sup> radical scavenging activity of GP films (44%) which still maintained  
719 constant despite of increasing heating temperature. For GP-glu films, an increase of about  
720 37% has been noted only for GP-glu films heated at 90 °C. Beyond 90 °C, there is no  
721 significant difference in terms of ABTS<sup>+</sup> radical scavenging activity between G, GP and GP-  
722 glu films. You, Luo, Shen, & Song (2011) reported that the ABTS radical scavenging activity  
723 of silver carp protein hydrolysate–glucose system obtained at 60 °C was significantly higher  
724 than that those obtained at 50 °C. As observed for the DPPH• FRSA, the decrease of the  
725 ABTS<sup>+</sup> of GP-glu films heated at temperatures higher than 90 °C could be attributed to the  
726 increase of crosslinking degree that limits the molecular mobility and thus their release in the  
727 reaction medium.

#### 728 *3.4.3. Reducing power*

729 The reducing power has been used to evaluate the effect of heating temperature on the  
730 antioxidant activity of G, GP and GP-glu films (Fig. 8.C). This assay measures particularly  
731 the antioxidative activity of MRPs as the hydroxyl groups of MRPs play a role in the reducing  
732 activity through their redox potential of transferring electrons (Vhangani & Van Wyk, 2013).  
733 For the G and GP, the reducing power, evaluated by measuring the absorbance at 700 nm  
734 ( $OD_{700}$ ), was maintained constant for 90 °C heated GP films compared to non-heated G and  
735 GP films. The reducing power of GP films is slightly higher than the one of G films because  
736 plasticization enhanced the release of active compounds resulting of gelatin degradation into  
737 small peptides at temperatures higher than 110 °C. Regarding GP-glu films, their reducing  
738 capacity increased significantly as a function of MR temperature and reached its maximum  
739 ( $OD_{700} \approx 0.7$ ) at 100 °C. Loucif, Chetouani, Bounekhel & Elkolli (2017) reported that the

740 reducing power increase of gelatin-alginate system prepared at pH=11 correlated well with  
741 increasing MR temperature from 70 to 90 °C.

#### 742 3.4.4. *β-carotene-linoleate bleaching inhibition*

743 The  $\beta$ -carotene-linoleate bleaching inhibition assay was used to assess the antioxidant  
744 activity of prepared films. As shown in Fig. 8.D, NH-GP films exhibited the lowest  
745 antioxidant power (10%) which increased then to reach only 18% at 130 °C. For GP-glu  
746 films, a significant increase of the antioxidant activity has been obtained when heating  
747 temperature increases. The generated MRPs could hinder the extent of  $\beta$ -carotene bleaching  
748 by neutralizing the linoleate-free radicals formed in the emulsion system, and the activity  
749 reached 18%, 22%, 28%, 35% and 43% for 90, 100, 110, 120 and 130 °C heated films,  
750 respectively. Additionally, as can be noticed, the antioxidant activity increased with  
751 increasing the browning intensity (expressed as  $A_{420nm}$ , Fig. 5.B). Thus, the enhancement of  
752 the  $\beta$ -carotene bleaching prevention correlate well with the elaboration of the brown colored  
753 MRPs in relation with the increase of heating temperature.

#### 754 3.4.5. *Linoleic acid oxidation inhibition*

755 Lastly, the inhibition of the *in-vitro* linoleic acid oxidation of GP and GP-glu films  
756 heated at different temperatures was investigated and results are presented in Fig. 8.E. The  
757 lipid peroxidation is the oxidative alteration of polyunsaturated fatty acids in cell membranes.  
758 It leads to the appearance of several degradation products including malondialdehyde (MDA)  
759 which is one of the several low-molecular-weight final products formed via the  
760 decomposition of certain primary and secondary lipid peroxidation products. Indeed, the  
761 MDA is widely studied as a marker of oxidative stress and index of lipid peroxidation  
762 (Janero, 1990). As displayed in Fig. 8.E1 and 8.E2, both of glucose-free gelatin (GP) and  
763 gelatin-glucose (GP-glu) films inhibited the MDA formation during linoleic acid storage

764 under heating conditions. These results prove the ability of films to donate an hydrogen atom  
765 to free radicals, leading to decelerate the propagation chain reaction rate occurred during lipid  
766 oxidation process (Abdelhedi et al., 2016). As can be seen, the antioxidant activity increased  
767 with increasing the incubation time and reached its maximum at the 7<sup>th</sup> day. The revealed  
768 antioxidant activity values extended 69.01%, 70.51%, 76.47%, 76.52% and 75.83% for GP-  
769 glu films heated at 90, 100, 110, 120 and 130 °C, respectively. Then, a decrease in the  
770 antioxidant activity has been revealed at the 10<sup>th</sup> day for GP-glu films which reached 31.10%,  
771 49.38%, 54.13%, 51.85% and 55.37% after heat treatments at 90, 100, 110, 120 and 130°C,  
772 respectively. Regarding GP films, the decrease in the lipid peroxidation inhibition capacity  
773 was more noticeable. Such findings indicated that GP-glu films heated at  $T \geq 100$  °C are more  
774 effective than GP films. Thus, heated GP-glu films could be used as active packaging in order  
775 to retard the oxidative degradation by inhibiting free radicals.

### 776 3.5. Activation energy

777 The activation energy was determined for all the studied parameters. Plots and  
778 calculation displayed that the Arrhenius equation did not apply to the antioxidant properties as  
779 the  $R^2$  is not significant as displayed in the table 3 and supplementary data. However, we can  
780 claim that the Maillard reaction was favored by glucose addition. It always decreases the  
781 activation energy, except for the  $\beta$ -carotene bleaching inhibition. Indeed, for the latter, the  
782 experiment was conducted at 50°C, which greatly favored the diffusion and thus the release of  
783 the MRPs having the greatest bleaching inhibition activity.

784

785 The  $R^2$  were significant ( $\geq 0.8$ ) for all the studied parameters except those related to  
786 antioxidant data. The activation energies of crosslinking degrees are respectively 23.3 kJ/mol  
787 and 16.1 kJ/mol for GP and GP-glu films. Glucose thus makes the cross-linking easier as it  
788 requires less energy. This is logical as cross-linking results of MR were enhanced by glucose.

789 This is in line with the color parameters indicating the Maillard reaction degree. Indeed,  $\Delta E$ -  
790 values for GP films require 5 times more energy than the one containing glucose as the  $E_a$   
791 varied from 25 to 122.1 kJ/mol (table 3, supplementary data). To confirm color change  
792 according temperature, the UV-Visible properties were also considered. Arrhenius  
793 representations (supplementary data) of the absorbance at 294 nm which indicates the  
794 presence of the intermediate MRPs, clearly display the change in activation energy below and  
795 above 120 °C, and the  $E_a$  rose respectively from 24.1 to 133.8 kJ/mol for the GP films.  
796 Furthermore, the  $E_a$  was higher in the case of GP films compared to GP-glu films in the case  
797 of  $A_{294\text{nm}}$  and  $A_{420\text{nm}}$  values (Table 3).

798 Additionally, results displayed that the water solubility activation energy of GP-glu  
799 films was reduced indicating that glucose addition made the enhancement of water  
800 sensitivity of films easier, especially in the range of 90-100 °C (as revealed by Arrhenius plot  
801 given in the supplementary data). Indeed, the  $E_a$  decreased from -5.0 kJ/mol to -59.8 kJ/mol  
802 for GP films and GP-glu films, respectively.

#### 803 **4. Conclusion**

804 A significant decrease of water solubility and an increase of UV-barrier ability were  
805 observed for gelatin-glucose films heated for 24 h at different temperatures (90-130 °C). The  
806 addition of glycerol and of glucose allowed to preventing more the gelatin hydrolysis during  
807 heating treatment. Indeed, an increase of thermal stability and a variation of structural  
808 properties have been revealed for gelatin-glucose films by means of XRD, TGA and DSC  
809 results. Prepared films showed an interesting antioxidant potential as evidenced by the  
810 reducing power, the DPPH• and the ABTS<sup>+</sup> radicals scavenging assays, the  $\beta$ -carotene-  
811 linoleate bleaching inhibition as well as the linoleic acid oxidation inhibition assays. Glucose-  
812 gelatin films heated at high temperatures showed antioxidant potential with different modes of  
813 actions (electron transfer, hydrogen atom donation). Regarding the heating temperature effect,

814 it appears clear that 90 °C seems to be enough to improve the antioxidant activity of gelatin  
815 films as evidenced by the different *in-vitro* assays. On the other hand, the thermal treatment  
816 ( $T \geq 100$  °C) alone can be a useful tool for enhancing the antioxidant activity of glucose-free  
817 gelatin films. Therefore, the Maillard reaction leads to generate bioactive compounds, which  
818 confer functional and satisfactory properties to gelatin films, which are suitable for the  
819 application as food packaging.

## 820 **Acknowledgements**

821 The co-tutelle PhD of Ms Kchaou is supported by the Utique PHC program (project  
822 SeaCoatPack) N° 39290YK of Campus France and N° 18G0903 of the CMCU funded by the  
823 Ministries of Education and Research of both France and Tunisia and the French Embassy in  
824 Tunisia. The authors wish to thank the colleagues from the PAM-PAPC Laboratory for  
825 precious collaboration and help, and to thank ESIREM (Engineering School of Materials of  
826 the Université de Bourgogne) for the facilitated accessibility to equipment and devices. This  
827 work was also supported by the Regional Council of Bourgogne –Franche Comté and the  
828 "Fonds Européen de Développement Régional (FEDER)" who invested in equipments.

829

## 830 **References**

- 831 Abdelhedi, O., Jridi, M., Jemil, I., Mora, L., Toldrá, F., Aristoy, M.-C., Boualga, A., Nasri,  
832 M., & Nasri, R. (2016). Combined biocatalytic conversion of smooth hound viscera:  
833 Protein hydrolysates elaboration and assessment of their antioxidant, anti-ACE and  
834 antibacterial activities. *Food Research International*, 86, 9-23.
- 835 Abdelhedi, O., Nasri, R., Jridi, M., Kchaou, H., Nasreddine, B., Karbowskiak, T., Debeaufort,  
836 F., & Nasri, M. (2018). Composite bioactive films based on smooth-hound viscera

837 proteins and gelatin: Physicochemical characterization and antioxidant properties.  
838 *Food Hydrocolloids*, 74(Supplement C), 176-186.

839 Alfaro, A. d. T., Balbinot, E., Weber, C. I., Tonial, I. B., & Machado-Lunkes, A. (2015). Fish  
840 Gelatin: Characteristics, functional properties, applications and future potentials. *Food*  
841 *Engineering Reviews*, 7(1), 33-44.

842 Amarowicz, R. (2009). Antioxidant activity of Maillard reaction products. *European Journal*  
843 *of Lipid Science and Technology*, 111(2), 109-111.

844 BenBettaïeb, N., Karbowski, T., Bornaz, S., & Debeaufort, F. (2015). Spectroscopic analyses  
845 of the influence of electron beam irradiation doses on mechanical, transport properties  
846 and microstructure of chitosan-fish gelatin blend films. *Food Hydrocolloids*, 46, 37-  
847 51.

848 Bergo, P., & Sobral, P. J. A. (2007). Effects of plasticizer on physical properties of pigskin  
849 gelatin films. *Food Hydrocolloids*, 21(8), 1285-1289.

850 Bubnis, W. A., & Ofner, C. M. (1992). The determination of  $\epsilon$ -amino groups in soluble and  
851 poorly soluble proteinaceous materials by a spectrophotometric method using  
852 trinitrobenzenesulfonic acid. *Analytical Biochemistry*, 207(1), 129-133.

853 Caoa, N., Fua, Y., & Hea, J. (2007). Preparation and physical properties of soy protein isolate  
854 and gelatin composite films. *Food Hydrocolloids*, 21, 1153-1162.

855 Cerny, C., & Guntz-Dubini, R. (2006). Role of the solvent glycerol in the Maillard reaction of  
856 D-fructose and L-alanine. *Journal of Agricultural and Food Chemistry*, 54 (2), 574-  
857 577.

858 Delgado-Andrade, C., Seiquer, I., Haro, A., Castellano, R., & Navarro, M. P. (2010).  
859 Development of the Maillard reaction in foods cooked by different techniques. Intake  
860 of Maillard-derived compounds. *Food Chemistry*, 122(1), 145-153.

861 Duconseille, A., Astruc, T., Quintana, N., Meersman, F., & Sante-Lhoutellier, V. (2015).  
862 Gelatin structure and composition linked to hard capsule dissolution: A review. *Food*  
863 *Hydrocolloids*, 43, 360-376.

864 Etxabide, A., Urdanpilleta, M., de la Caba, K., & Guerrero, P. (2016). Control of cross-  
865 linking reaction to tailor the properties of thin films based on gelatin. *Materials*  
866 *Letters*, 185, 366-369.

867 Etxabide, A., Urdanpilleta, M., Gómez-Arriaran, I., de la Caba, K., & Guerrero, P. (2017).  
868 Effect of pH and lactose on cross-linking extension and structure of fish gelatin films.  
869 *Reactive and Functional Polymers*, 117(Supplement C), 140-146.

870 Etxabide, A., Vairo, C., Santos-Vizcaino, E., Guerrero, P., Pedraz, J. L., Igartua, M., de la  
871 Caba, K., & Hernandez, R. M. (2017). Ultra thin hydro-films based on lactose-  
872 crosslinked fish gelatin for wound healing applications. *International Journal of*  
873 *Pharmaceutics*, 530(1), 455-467.

874 Ge, L., Zhu, M., Li, X., Xu, Y., Ma, X., Shi, R., Li, D., & Mu, C. (2018). Development of  
875 active rosmarinic acid-gelatin biodegradable films with antioxidant and long-term  
876 antibacterial activities. *Food Hydrocolloids*, 83, 308-316.

877 Gennadios, A., Handa, A., Froning, G. W., Weller, C. L., & Hanna, M. A. (1998). Physical  
878 Properties of egg white–dialdehyde starch films. *Journal of Agricultural and Food*  
879 *Chemistry*, 46(4), 1297-1302.

880 Gennadios, A., Ghorpade, V. M., Weller, C. L., & Hanna, M. A. (1996). Heat curing of soy  
881 protein films. *Transactions of the ASAE*, 39, 575–579.

882 González Seligra, P., Medina Jaramillo, C., Famá, L., Goyanes, S. (2016). Data of thermal  
883 degradation and dynamic mechanical properties of starch–glycerol based films with  
884 citric acid as crosslinking agent. *Data in Brief*, 7, 1331–1334.

885 Hoff, M. J. H. v. t. (1884). Etudes de dynamique chimique. *Recueil des Travaux Chimiques*  
886 *des Pays-Bas*, 3(10), 333-336.

887 Hoque, M. S., Benjakul, S., & Prodpran, T. (2010). Effect of heat treatment of film-forming  
888 solution on the properties of film from cuttlefish (*Sepia pharaonis*) skin gelatin.  
889 *Journal of Food Engineering*, 96, 66–73.

890 Hoque, M. S., Benjakul, S., & Prodpran, T. (2011). Effects of partial hydrolysis and  
891 plasticizer content on the properties of film from cuttlefish (*Sepia pharaonis*) skin  
892 gelatin. *Food Hydrocolloids*, 25(1), 82-90.

893 Janero, D. R. (1990). Malondialdehyde and thiobarbituric acid-reactivity as diagnostic indices  
894 of lipid peroxidation and peroxidative tissue injury. *Free Radic Biol Med*, 9(6), 515-  
895 540.

896 Jiang, Z., Wang, L., Che, H., & Tian, B. (2014). Effects of temperature and pH on  
897 angiotensin-I-converting enzyme inhibitory activity and physicochemical properties of  
898 bovine casein peptide in aqueous Maillard reaction system. *LWT - Food Science and*  
899 *Technology*, 59(1), 35-42.

900 Jridi, M., Sellimi, S., Lassoued, K. B., Beltaief, S., Souissi, N., Mora, L., Toldra, F., Elfeki,  
901 A., Nasri, M., & Nasri, R. (2017). Wound healing activity of cuttlefish gelatin gels and  
902 films enriched by henna (*Lawsonia inermis*) extract. *Colloids and Surfaces A:*  
903 *Physicochemical and Engineering Aspects*, 512, 71-79.

904 Jridi, M., Hajji, S., Ben Ayed, I., Lassoued, I., Mbarek, A., Kammoun, M., Souissi, N., Nasri,  
905 M.(2014). Physical, structural, antioxidant and antimicrobial properties of gelatin–  
906 chitosan composite edible films, *International Journal of Biological Macromolecules*, 67  
907 373-379.

908 Julius, A. (1967). Food wrapping membrane. U.S. Patent 3,329,509.

909 Kaanane, A., & Labuza, T. P. (1989). The Maillard reaction in foods. In J. Baynes (Ed.), The  
910 Maillard reaction in aging, diabetes and nutrition (pp. 301–327). New York, NY,  
911 USA: A.R. Liss Press, Inc.

912 Karseno, E., Yanto, T., Setyowati, R., & Haryanti, P. (2018). Effect of pH and temperature on  
913 browning intensity of coconut sugar and its antioxidant activity. *Food Research*, 2(1),  
914 32-38.

915 Kchaou, H., Benbettaïeb, N., Jridi, M., Abdelhedi, O., Karbowiak, T., Brachais, C.-H.,  
916 Léonard, M.-L., Debeaufort, F., & Nasri, M. (2018). Enhancement of structural,  
917 functional and antioxidant properties of fish gelatin films using Maillard reactions.  
918 *Food Hydrocolloids*, 83, 326-339.

919 Kim, K. M.; Weller, C. L.; Hanna, M. A.; Gennadios, A. (2002). Heat curing of soy protein  
920 films at selected temperatures and pressures. *Lebensmittel-Wissenschaft und-*  
921 *Technologie* , 35, 140–145.

922 Koleva, I. I., van Beek, T. A., Linssen, J. P. H., de Groot, A., & Evstatieva, L. N. (2002).  
923 Screening of plant extracts for antioxidant activity: a comparative study on three  
924 testing methods. *Phytochemical Analysis*, 13, 8-17.

925 Labuza, T. P. (1984). Application of chemical kinetics to deterioration of foods. *Journal of*  
926 *Chemical Education*, 61, 348–358.

927 Labuza, T. P., & Baisier, W. M. (1992). The kinetics of nonenzymatic browning. In H.  
928 Schwartzberg, & R. Hartel (Eds.), *Physical chemistry of foods* (pp. 595–649). New  
929 York, NY, USA: Marcel Dekker.

930 Labuza, T. P., & Saltmarch, M. (1981). The nonenzymatic browning reaction as affected by  
931 water in foods. In L. Rockland, & G. F. Stewart (Eds.), *Water activity influences on*  
932 *food quality* (pp. 605–650). New York, NY, USA: Academic Press.

933 Lan, X., Liu, P., Xia, S., Jia, C., Mukunzi, D., Zhang, X., Xia, W., Tian, H., & Xiao, Z.  
934 (2010). Temperature effect on the non-volatile compounds of Maillard reaction  
935 products derived from xylose–soybean peptide system: Further insights into thermal  
936 degradation and cross-linking. *Food Chemistry*, 120(4), 967-972.

937 Leceta, I., Guerrero, P., & de la Caba, K. (2013a). Functional properties of chitosan based  
938 films. *Carbohydrate Polymers*, 93, 339-346.

939 Leceta, I., Guerrero, P., Ibarburu, I., Duenas, M. T., & de la Caba, K. (2013b).  
940 Characterization and antimicrobial analysis of chitosan-based films. *Journal of Food*  
941 *Engineering*, 116, 889-899.

942 Li, H., Liu, B. L., Gao, L. Z., & Chen, H. L. (2004). Studies on bullfrog skin collagen. *Food*  
943 *Chemistry*, 84(1), 65-69.

944 Liu, F., Majeed, H., Antoniou, J., Li, Y., Ma, Y., Yokoyama, W., Ma, J., & Zhong, F. (2016).  
945 Tailoring physical properties of transglutaminase-modified gelatin films by varying  
946 drying temperature. *Food Hydrocolloids*, 58, 20-28.

947 Liu, J., Liu, M., He, C., Song, H., & Chen, F. (2015). Effect of thermal treatment on the flavor  
948 generation from Maillard reaction of xylose and chicken peptide. *LWT - Food Science*  
949 *and Technology*, 64(1), 316-325.

950 Loucif K., Chetouani A., Bounekhel M., &Elkolli M. (2017). Alginate/gelatin crosslinked  
951 system through Maillard reaction: preparation, characterization and biological  
952 properties. *Polymer Bulletin*, 74(12), 4899-4919.

953 Maillard, M. N., Billaud, C., Chow, Y. N., Ordonaud, C., & Nicolas, J. (2007). Free radical  
954 scavenging, inhibition of polyphenoloxidase activity and copper chelating properties  
955 of model Maillard systems. *LWT - Food Science and Technology*, 40(8), 1434-1444.

956 Miller, K. S., Chiang, M. T., & Krochta, J. M. (1997). Heat curing of whey protein films.  
957 *Journal of Food Science*, 62, 1189–1193.

958 Nasrollahzadeh, F., Varidi, M., Koocheki, A., & Hadizadeh, F. (2017). Effect of microwave  
959 and conventional heating on structural, functional and antioxidant properties of bovine  
960 serum albumin-maltodextrin conjugates through Maillard reaction. *Food Research*  
961 *International*, 100, 289-297.

962 Osawa, T., & Namiki, M. (1985). Natural antioxidants isolated from Eucalyptus leaf waxes.  
963 *Journal of Agricultural and Food Chemistry*, 33(5), 777-780.

964 Pirestani, S., Nasirpour, A., Keramat, J., Desobry, S., & Jasniewski, J. (2018). Structural  
965 properties of canola protein isolate-gum Arabic Maillard conjugate in an aqueous  
966 model system. *Food Hydrocolloids*, 79, 228-234.

967 Prasertsung, I., Mongkolnavin, R., Kanokpanont, S., & Damrongsakkul, S. (2010). The  
968 effects of pulsed inductively coupled plasma (PICP) on physical properties and  
969 biocompatibility of crosslinked gelatin films. *International Journal of Biological*  
970 *Macromolecules*, 46(1), 72-78.

971 Poppe, J. (1997). Gelatin. In: *Thickening and Gelling Agents for Food* (edited by A. Imeson).  
972 London: Blackie Academic and Professional, 144–168.

973 Re, R., Pellegrini, N., Proteggente, A., Pannala, A., Yang, M., & Rice-Evans, C. (1999).  
974 Antioxidant activity applying an improved ABTS radical cation decolorization assay.  
975 *Free Radical Biology and Medicine*, 26(9), 1231-1237.

976 Rhim, J. W., Gennadios, A., Handa, A., Weller, C. L., and Hanna, M. A. (2000). Solubility,  
977 tensile, and color properties of modified soy protein isolate films. *Journal of*  
978 *Agricultural Food Chemistry*, 48, 4937–4941.

979 Rivero, S., García, M. A., & Pinotti, A. (2012). Heat treatment to modify the structural and  
980 physical properties of chitosan-based films. *Journal of Agricultural and Food*  
981 *Chemistry*, 60, 492-499.

982 Simperler, A., Kornherr, A., Chopra, R., Bonnet, P. A., Jones, W., Motherwell, W. D. S.,  
983 (2006). Glass transition temperature of glucose, sucrose, and Trehalose:an  
984 experimental and in silico study. *The Journal of Physical Chemistry B*, 110(39),  
985 19678-19684.

986 Smarrito-Menozzi, C., Matthey-Dorret, W., Devaud-Goumoens, S., & Viton, F. (2013).  
987 Glycerol, an underestimated flavor precursor in the Maillard reaction. *Journal of*  
988 *Agricultural and Food Chemistry*, 61, 10225-10230.

989 Sun, Q., & Luo, Y. (2011). Effect of Maillard reaction conditions on radical scavenging  
990 activity of porcine haemoglobin hydrolysate–sugar model system. *International*  
991 *Journal of Food Science & Technology*, 46(2), 358-364.

992 Vhangani, L. N., & Van Wyk, J. (2013). Antioxidant activity of Maillard reaction products  
993 (MRPs) derived from fructose–lysine and ribose–lysine model systems. *Food*  
994 *Chemistry*, 137(1), 92-98.

995 Yagi, K. (1976). A simple fluorometric assay for lipoperoxide in blood plasma. *Biochemical*  
996 *Medicine*, 15(2), 212-216.

997 Yasir, B.M., Sutton, K.H., Newberry, M.P., Andrews, N.R.,& Gerardard, J.A.( 2007). The  
998 impact of Maillard crosslinking on soy proteins ad tofu texture. *Food Chemistry*, 104  
999 (4), 1502–1508.

1000 Yildırım, A., Mavi, A., & Kara, A. A. (2001). Determination of antioxidant and antimicrobial  
1001 activities of rumex crispus L. Extracts. *Journal of Agricultural and Food Chemistry*,  
1002 49(8), 4083-4089.

1003 You, J., Luo, Y., Shen, H., & Song, Y. (2011). Effect of substrate ratios and temperatures on  
1004 development of Maillard reaction and antioxidant activity of silver carp  
1005 (*Hypophthalmichthys molitrix*) protein hydrolysate–glucose system. *International*  
1006 *Journal of Food Science & Technology*, 46(12), 2467-2474.

- 1007 Yu, M., He, S., Tang, M., Zhang, Z., Zhu, Y., & Sun, H. (2018). Antioxidant activity and  
1008 sensory characteristics of Maillard reaction products derived from different peptide  
1009 fractions of soybean meal hydrolysate. *Food Chemistry*, 243, 249-257.
- 1010 Zhang, Z., Elfalleh, W., He, S., Tang, M., Zhao, J., Wu, Z., Wang, J., & Sun, H. (2018)  
1011 .Heating and cysteine effect on physicochemical and flavor properties of soybean  
1012 peptide Maillard reaction products. *International Journal of Biological*  
1013 *Macromolecules*, 120, 2137-2146.
- 1014 Weadock, K., Olson, R. M., & Silver, F. H. (1984). Evaluation of collagen cross-linking  
1015 techniques. *Biomaterials, Medical DevicesArtificial Organs*, 11, 293–318.
- 1016

1 **Figure captions**

2 **Figure 1:** Degree of crosslinking of G, GP and GP-glu films heated at 90 °C, 100 °C, 110 °C,  
3 120 °C and 130 °C. <sup>a,b,c,d</sup>: values with different letters are significantly different at  $p < 0.05$  in  
4 terms of temperature. ( ■ GP films, ● GP-glu films, ◆ G films).

5 **Figure 2:** FTIR spectra of GP and GP-glu films heated at 90 °C, 100 °C, 110 °C, 120 °C and  
6 130 °C.

7 **Figure 3:** Images of GP and GP-glu films heated at different temperatures (90 °C, 100 °C,  
8 110 °C, 120 °C and 130 °C).

9 **Figure 4:** UV-vis spectra of GP and GP-glu films heated at different temperatures at 90 °C,  
10 100 °C, 110 °C, 120 °C and 130 °C.

11 **Figure 5:** A: Absorbance at 294 nm and B: at 420 nm of GP and GP-glu films heated at 90  
12 °C, 100 °C, 110 °C, 120 °C and 130 °C (<sup>a,b,c,d,e,f</sup> values with different letters are significantly  
13 different at  $p < 0.05$  on the temperature effect) ( ■ GP films, ● GP-glu films).

14 **Figure 6:** XRD patterns of GP and GP-glu films heated at 90 and 130 °C compared to non  
15 heated films.

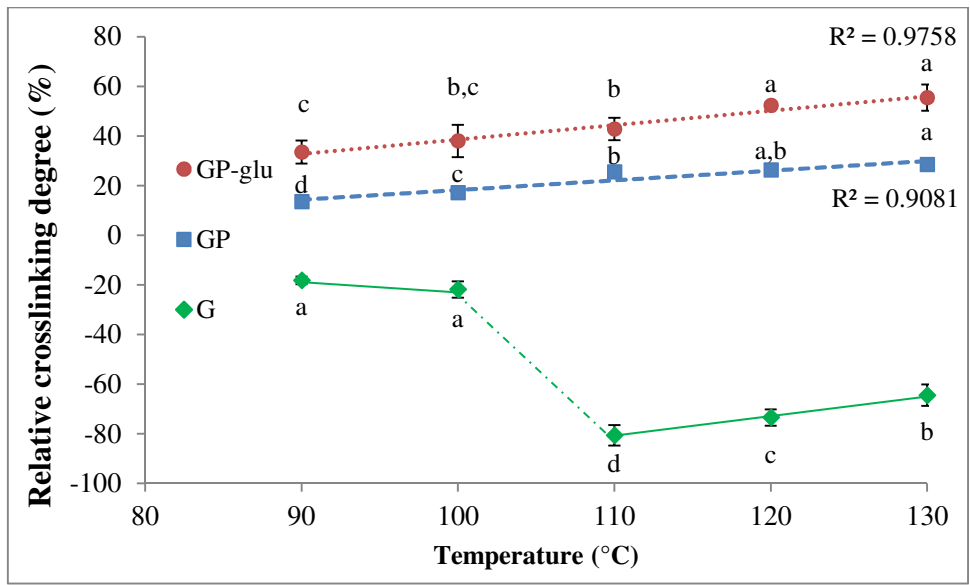
16 **Figure 7:** Water content (WC), water solubility and water contact angle (WCA) of GP and  
17 GP-glu films (and/or G films) heated at 90 °C, 100 °C, 110 °C, 120 °C and 130 °C (<sup>a,b,c</sup>  
18 significant difference ( $p < 0.05$ ) between temperature and  <sup>$\alpha,\beta,\gamma$</sup>  between films samples at a same  
19 temperature.) ( ■ GP films, ● GP-glu films, ◆ G films)

20 **Figure 8:** Antioxidant activity of GP and GP-glu films (and/or G films) heated at 90°C,  
21 100°C, 110°C, 120°C and 130°C assessed from the DPPH radical scavenging ability (A),  
22 ABTS<sup>+</sup> radical scavenging ability (B), reducing power (C),  $\beta$ -carotene bleaching inhibition  
23 (D) and lipid peroxidation inhibition capacity (E) tests (<sup>a,b,c,d,e</sup> values with different letters are  
24 significantly different at  $p < 0.05$  in terms of temperature,  <sup>$\alpha,\beta,\gamma$</sup>  values are significantly different  
25 at  $p < 0.05$  in terms of films sample for each temperature). ( ■ GP films, ● GP-glu films, ◆ G  
26 films)

27

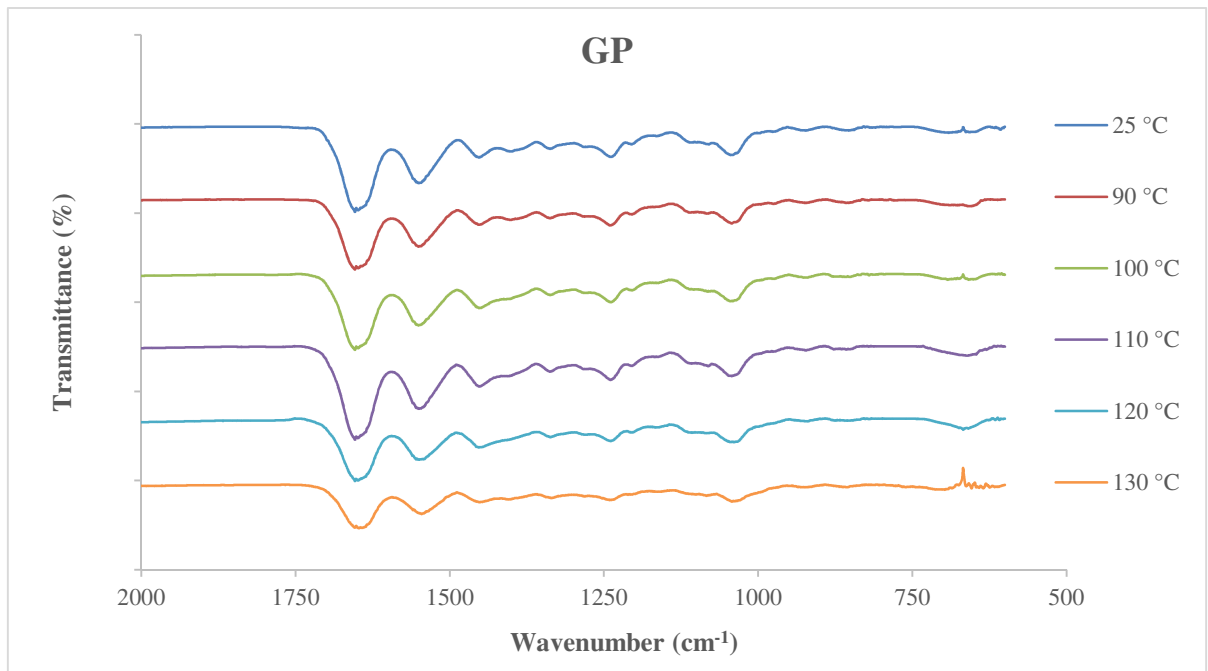
28 **Supplementary data:** Arrhenius plots for all film characteristics measured after heating at  
29 temperatures ranging from 90 to 130°C ( ■ GP films, ● GP-glu films, ◆ G films)

1 Fig. 1

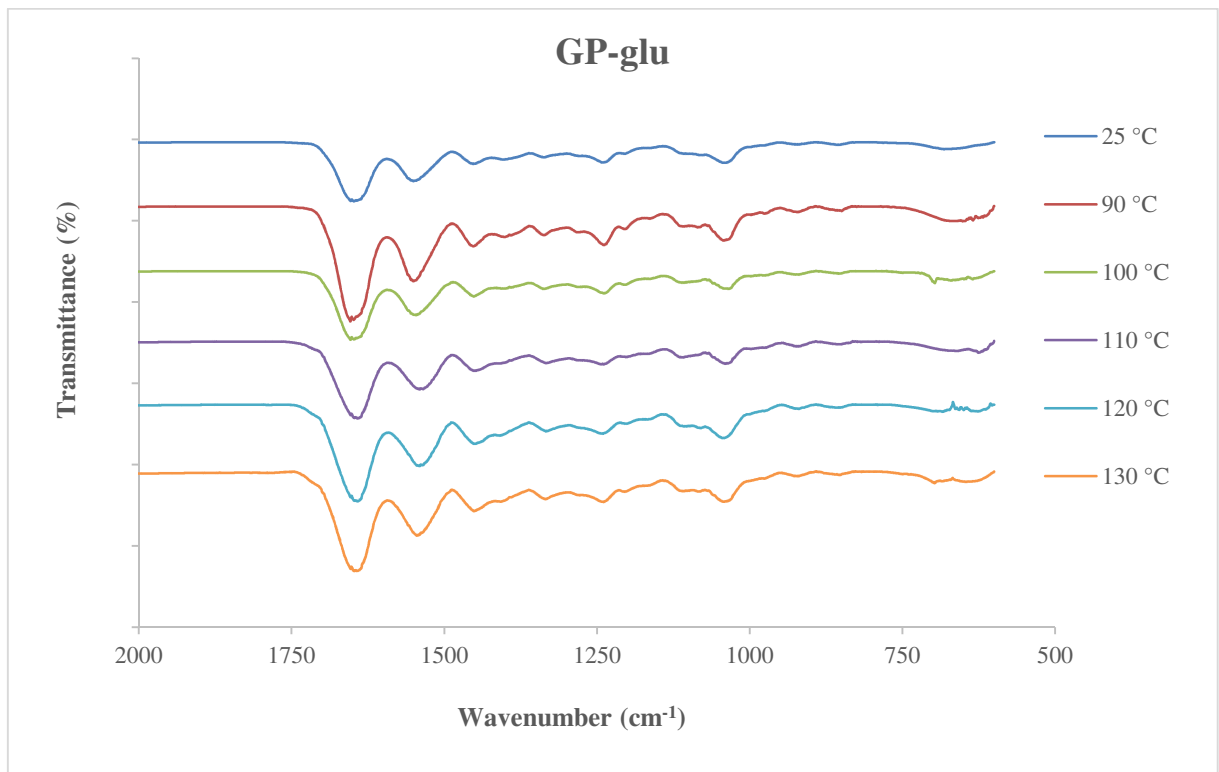


2

1 **Fig. 2**

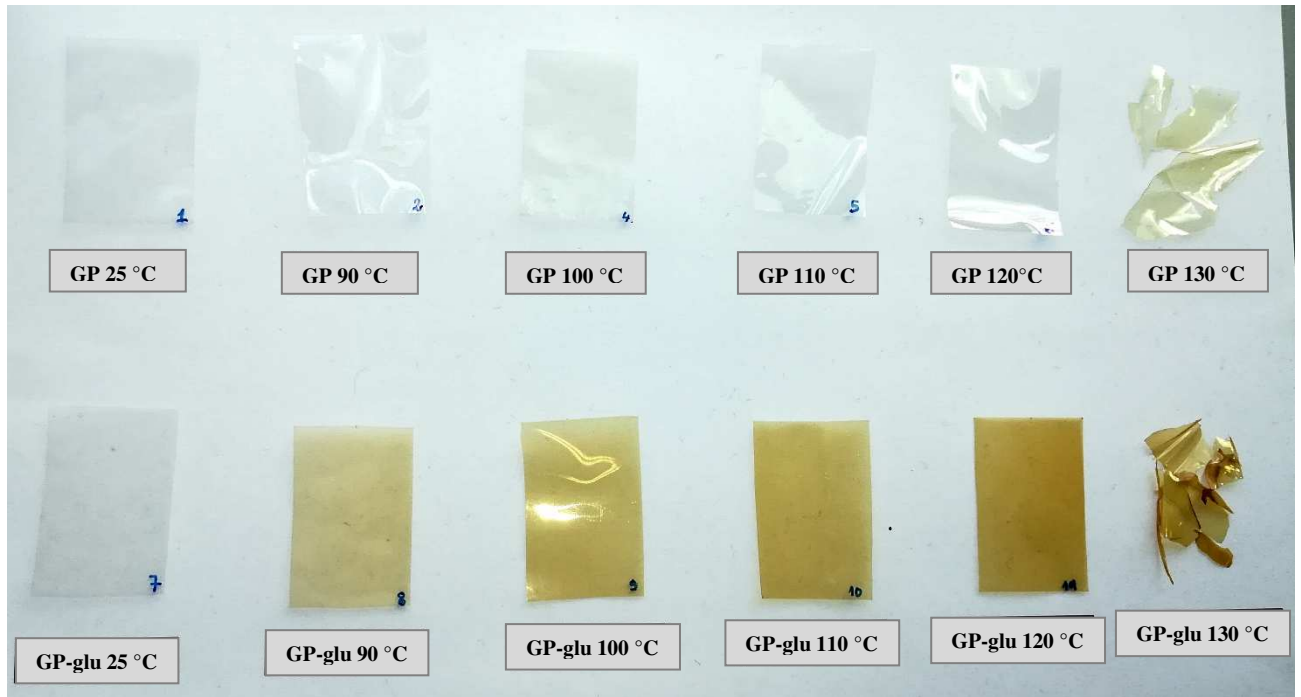


2



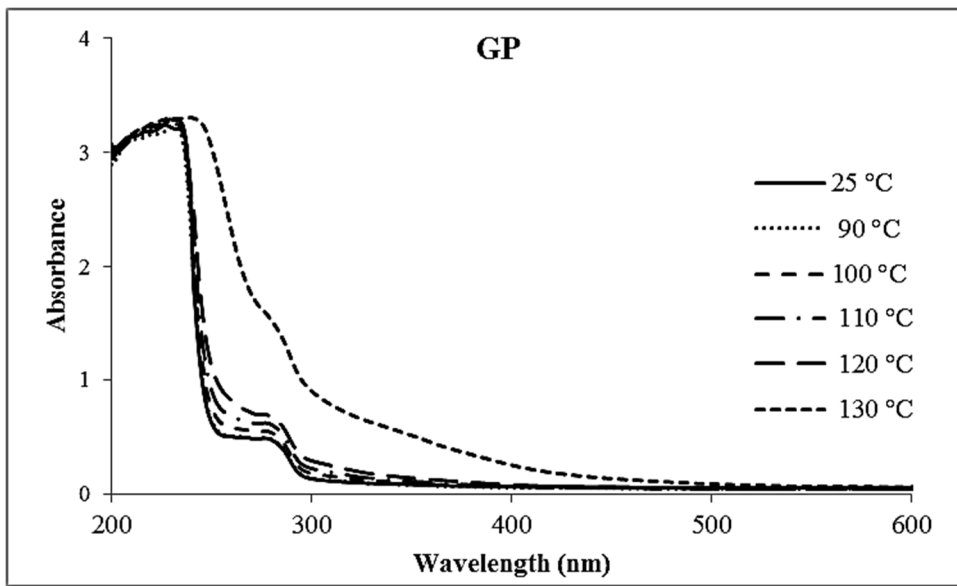
3

1 **Fig. 3**

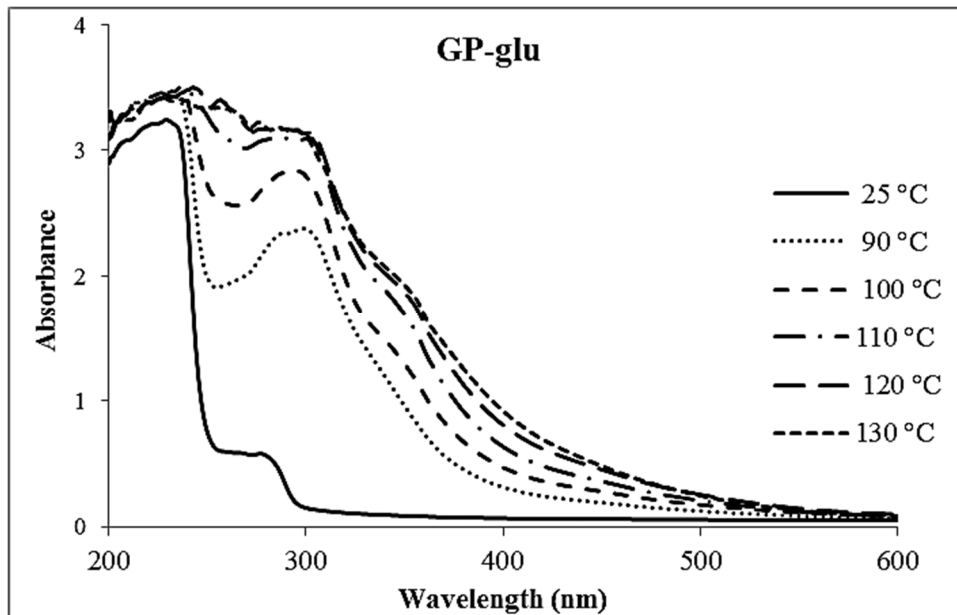


2

1 **Fig. 4**

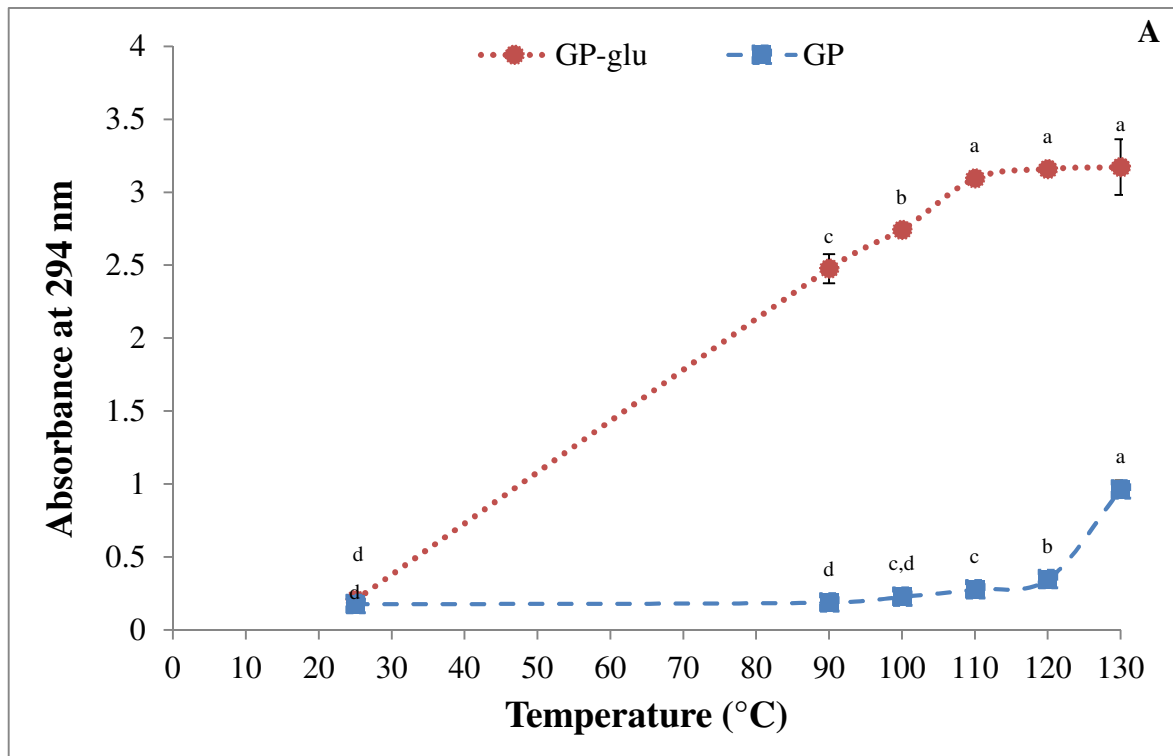


2



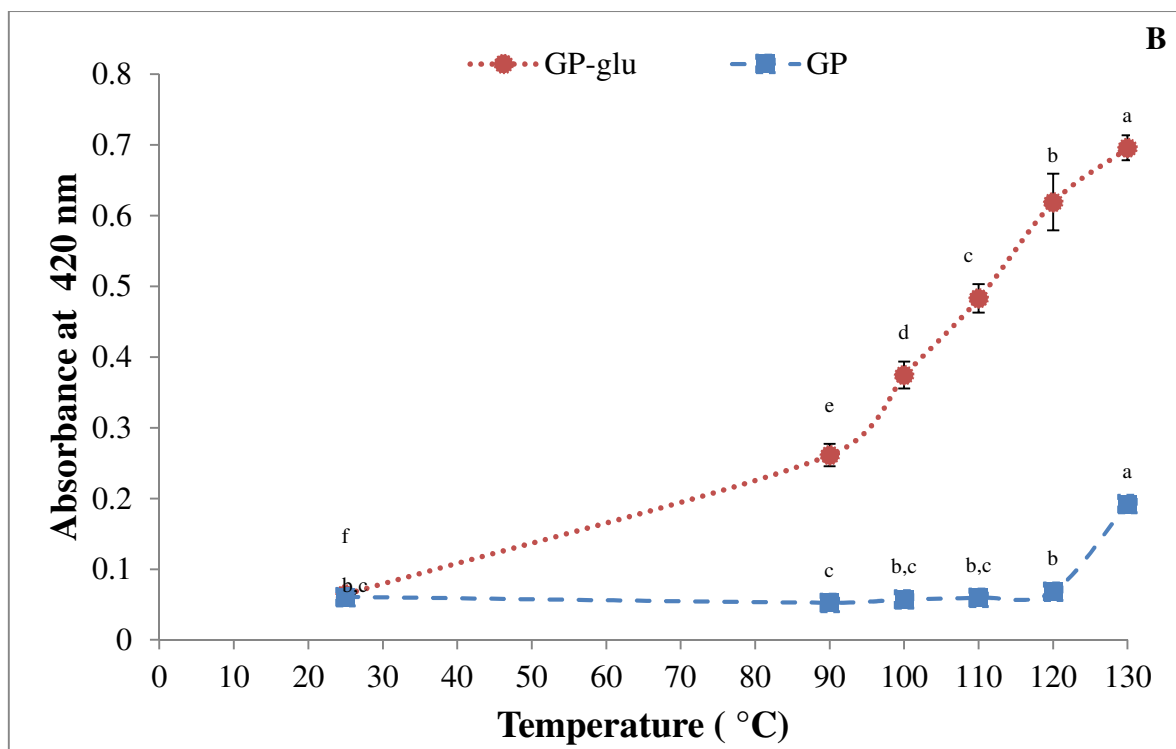
3

1 Fig. 5



2

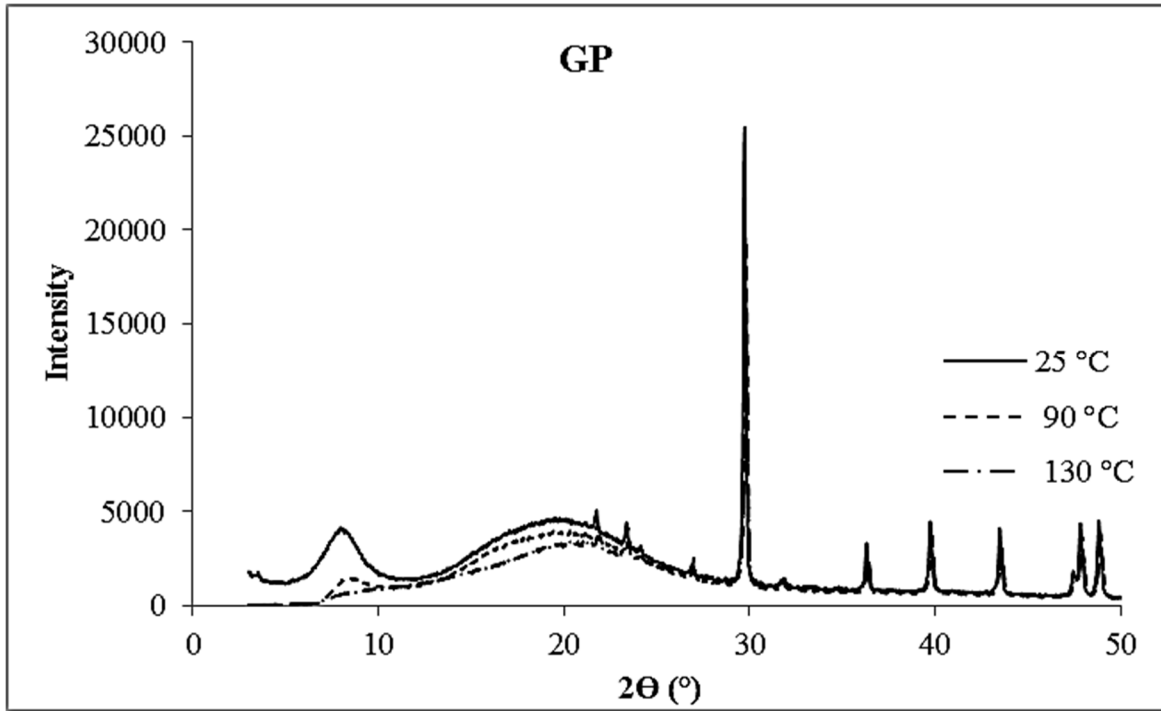
3



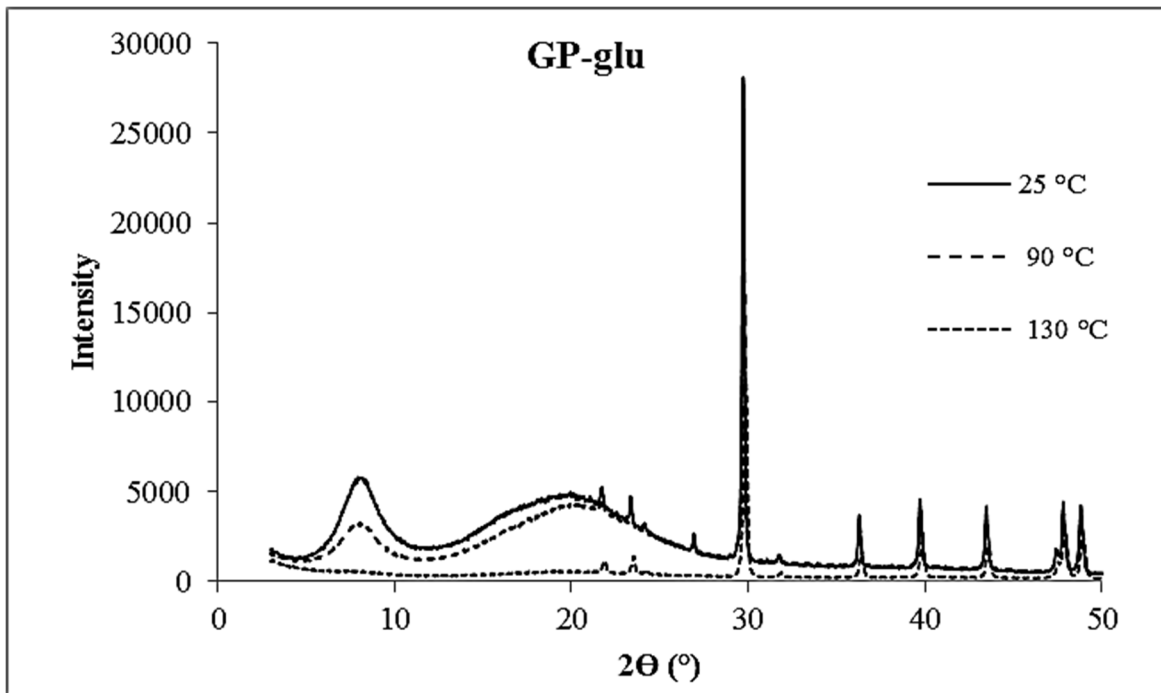
4

1 **Fig. 6**

2

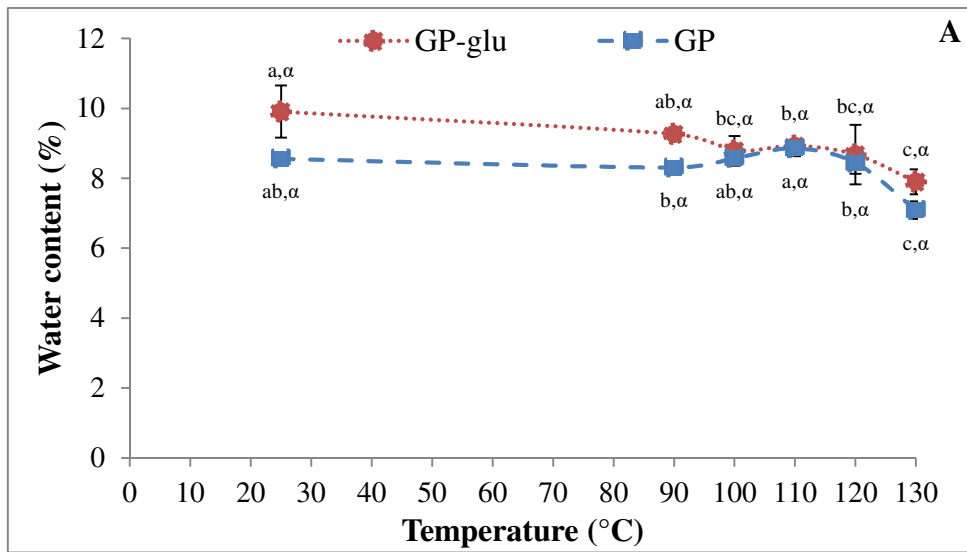


3

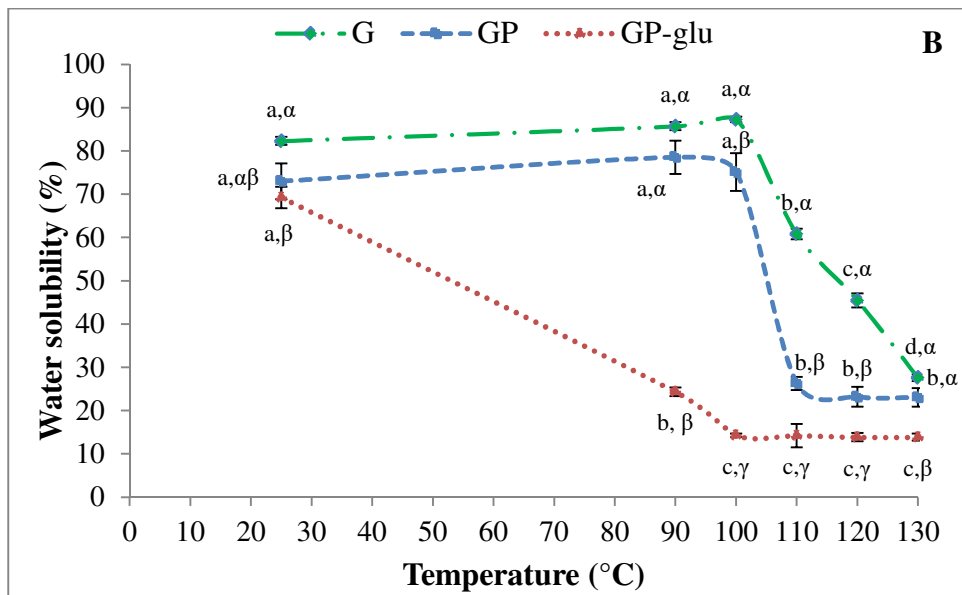


4

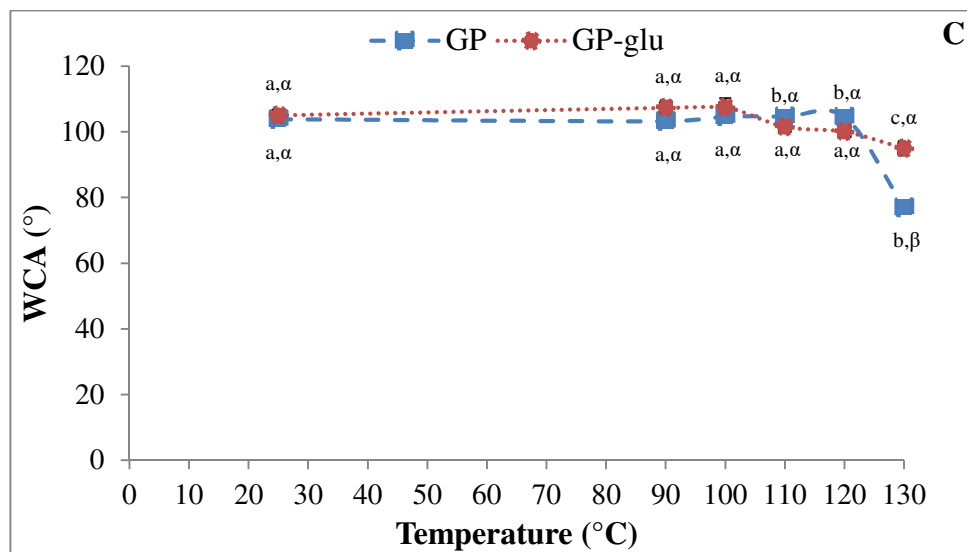
1 Fig. 7



2

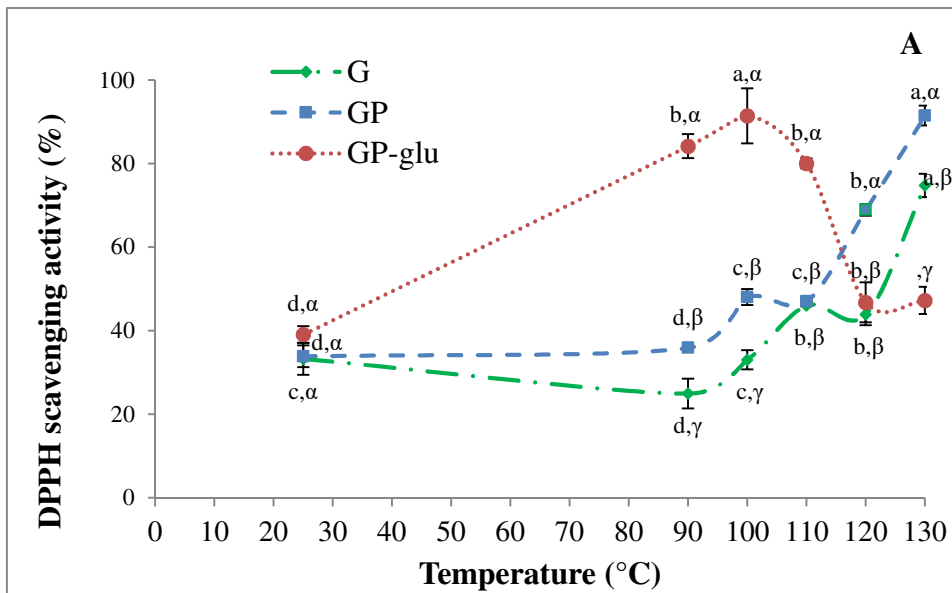


3

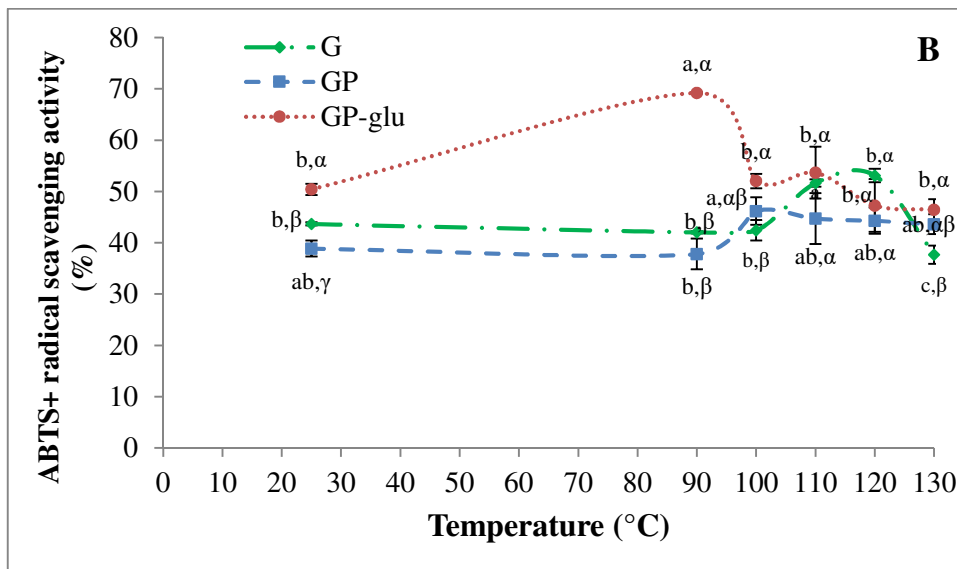


4

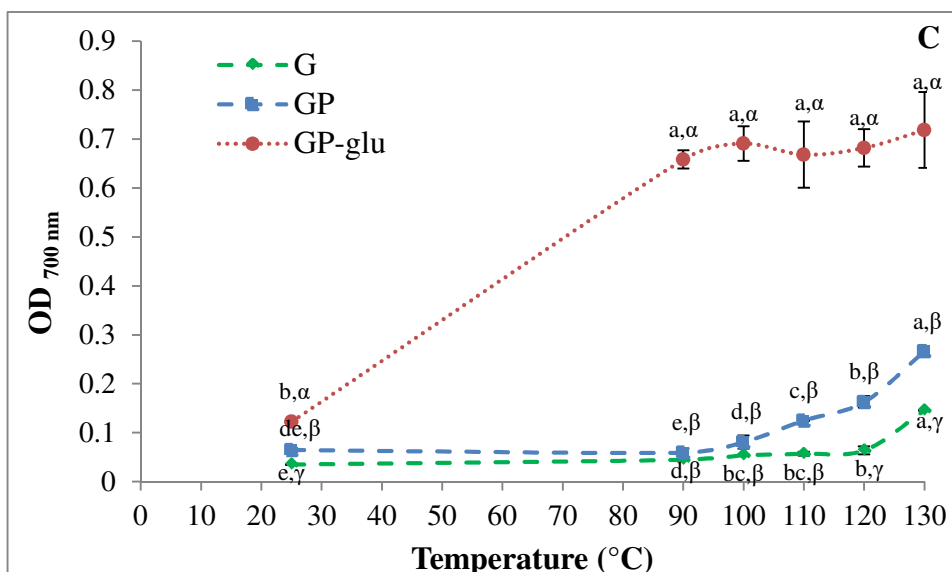
1 **Fig. 8**



2

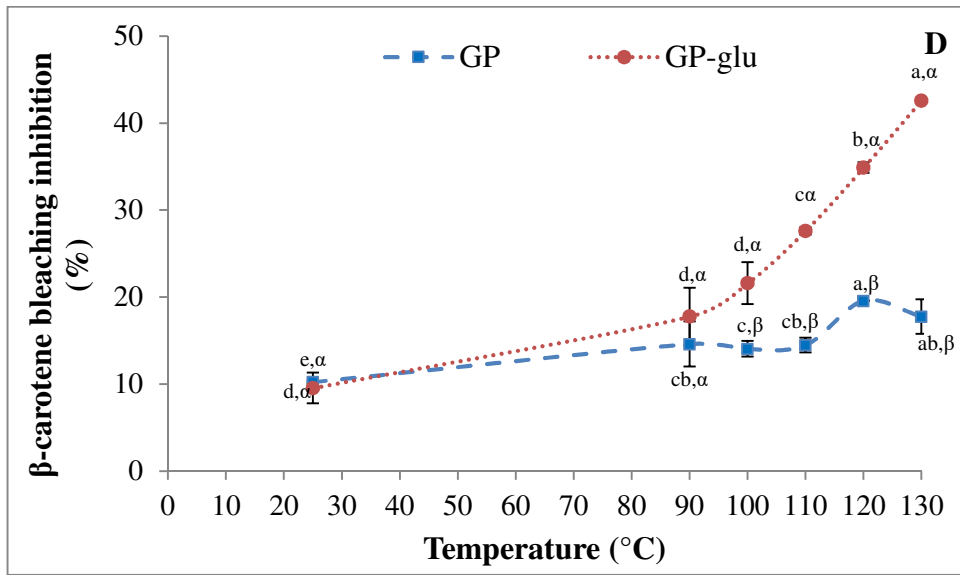


3

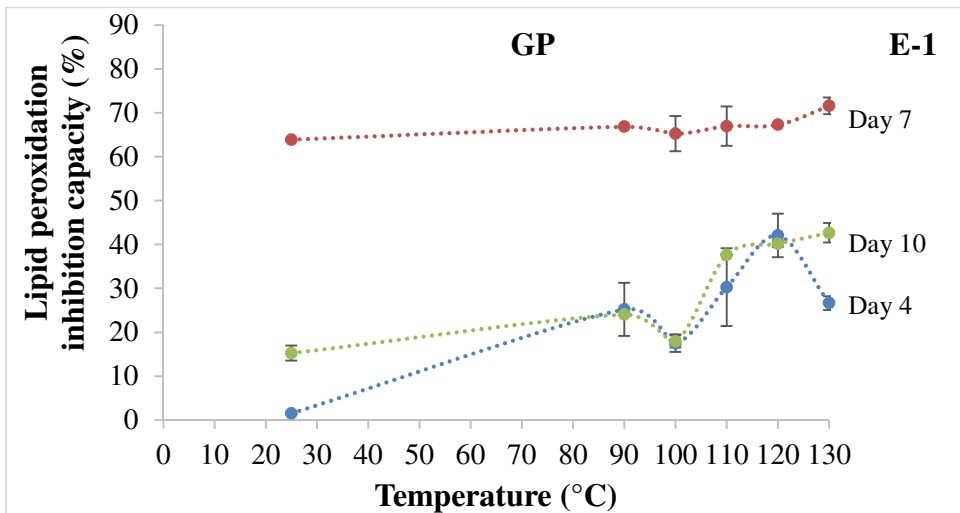


4

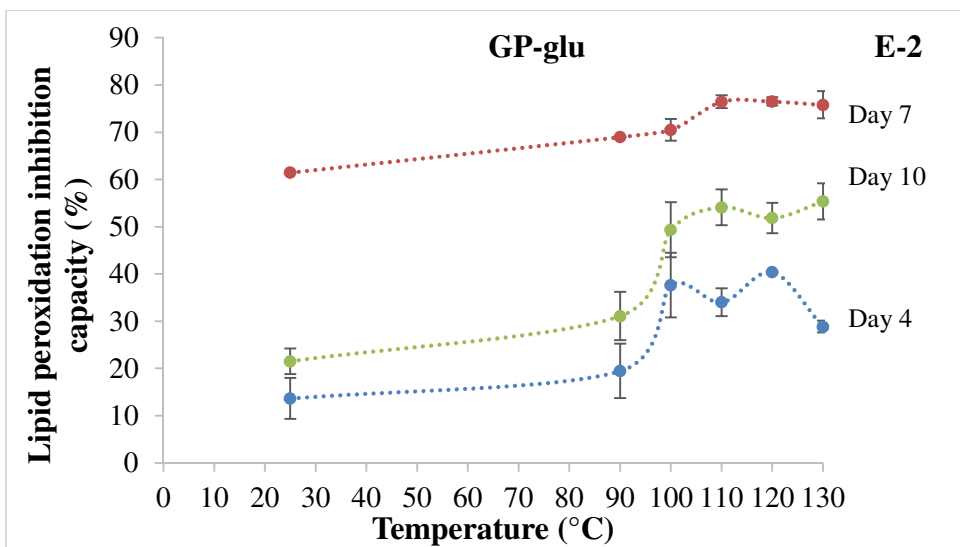
5



6



7



8

1 **Table 1:** Color parameters of GP and GP-glu films heated at different temperatures (90°C,  
 2 100°C, 110°C, 120°C and 130°C).

<b>Films</b>	<b>T (°C)</b>	<b>L</b>	<b>a</b>	<b>b</b>	<b>ΔE</b>	<b>BI</b>
<b>GP</b>	25	91.47 ± 0.06 <sup>a</sup>	1.47 ± 0.06 <sup>a</sup>	-3.87 ± 0.06 <sup>d</sup>	-	-
	90	91.40 ± 0.10 <sup>a</sup>	1.37 ± 0.06 <sup>a,b</sup>	-3.73 ± 0.06 <sup>d</sup>	0.21 ± 0.03 <sup>d</sup>	-
	100	91.50 ± 0.10 <sup>a</sup>	1.40 ± 0.10 <sup>a,b</sup>	-3.6 ± 0.10 <sup>d</sup>	0.30 ± 0.10 <sup>d</sup>	-
	110	91.53 ± 0.15 <sup>a</sup>	1.20 ± 0.10 <sup>b</sup>	-2.97 ± 0.06 <sup>c</sup>	0.96 ± 0.06 <sup>c</sup>	-
	120	91.23 ± 0.15 <sup>a</sup>	0.83 ± 0.06 <sup>c</sup>	-1.90 ± 0.17 <sup>b</sup>	2.09 ± 0.14 <sup>b</sup>	-
	130	90.60 ± 0.30 <sup>b</sup>	-2.83 ± 0.21 <sup>d</sup>	7.80 ± 0.46 <sup>a</sup>	12.47 ± 0.43 <sup>a</sup>	-
<b>GP-glu</b>	25	91.43 ± 0.06 <sup>a</sup>	1.43 ± 0.06 <sup>a</sup>	-3.83 ± 0.06 <sup>f</sup>	-	-
	90	87.07 ± 0.21 <sup>b</sup>	-1.83 ± 0.12 <sup>d</sup>	19.20 ± 0.72 <sup>e</sup>	5.85 ± 0.18 <sup>d</sup>	22.44 ± 1.10 <sup>e</sup>
	100	84.43 ± 0.15 <sup>c</sup>	-1.33 ± 0.06 <sup>c</sup>	29.70 ± 0.98 <sup>d</sup>	8.46 ± 0.13 <sup>c</sup>	40.42 ± 1.69 <sup>d</sup>
	110	80.53 ± 0.45 <sup>d</sup>	-1.2 ± 0.17 <sup>c</sup>	40.43 ± 1.50 <sup>c</sup>	12.31 ± 0.39 <sup>b</sup>	64.76 ± 3.14 <sup>c</sup>
	120	80.77 ± 0.35 <sup>d</sup>	-0.83 ± 0.12 <sup>b</sup>	44.33 ± 1.45 <sup>b</sup>	12.19 ± 0.36 <sup>b</sup>	73.85 ± 3.74 <sup>b</sup>
	130	79.60 ± 0.62 <sup>e</sup>	-1.33 ± 0.21 <sup>c</sup>	48.43 ± 2.89 <sup>a</sup>	13.47 ± 0.51 <sup>a</sup>	85.35 ± 6.93 <sup>a</sup>

3

4 ΔE: total color difference of GP and GP-glu films compared to their non heated films, respectively.

5 BI: browning index.

6 Different letters (a-f) in the same column within the same sample (GP or GP-glu) indicate significant  
 7 difference (p<0.05).

1 **Table 2:** Glass transition temperature ( $T_g$ ),  $C_p$  variation ( $\Delta C_p$ ) weight loss ( $\Delta w$ ),  
2 temperature of maximum degradation ( $T_{max}$ ) and residue of GP and GP-glu films heated at  
3 different temperatures (90°C, 100°C, 110°C, 120°C and 130°C).

Films	T (°C)	T <sub>g</sub> (°C)	$\Delta C_p$	$\Delta w$ (%)		T <sub>max</sub> (°C)	Residue (%)
				1st	2nd		
				transformation region	transformation region		
<b>G</b>	25	77 <sup>a</sup>	0.507 <sup>b</sup>	-	-	-	-
	90	83 <sup>a</sup>	0.534 <sup>ab</sup>	-	-	-	-
	100	83 <sup>a</sup>	0.508 <sup>b</sup>	-	-	-	-
	110	80 <sup>a</sup>	0.61 <sup>a</sup>	-	-	-	-
	120	78 <sup>a</sup>	0.502 <sup>b</sup>	-	-	-	-
	130	86 <sup>a</sup>	0.514 <sup>b</sup>	-	-	-	-
<b>GP</b>	25	51 <sup>b</sup>	0.511 <sup>a</sup>	5	77	306	18
	90	56 <sup>ab</sup>	0.306 <sup>c</sup>	6	70	311	24
	100	50 <sup>b</sup>	0.383 <sup>b</sup>	8	74	304	18
	110	56 <sup>ab</sup>	0.353 <sup>bc</sup>	6	70	304	25
	120	56 <sup>ab</sup>	0.217 <sup>d</sup>	5	72	312	24
	130	65 <sup>a</sup>	0.156 <sup>e</sup>	5	77	314	18
<b>GP- glu</b>	25	45 <sup>c</sup>	0.347 <sup>b</sup>	5	70	311	25
	90	52 <sup>bc</sup>	0.429 <sup>a</sup>	5	74	314	21
	100	55 <sup>ab</sup>	0.429 <sup>a</sup>	5	75	314	18
	110	59 <sup>ab</sup>	0.433 <sup>a</sup>	4	73	314	23
	120	59 <sup>ab</sup>	0.402 <sup>ab</sup>	8	70	314	22
	130	64 <sup>a</sup>	0.455 <sup>a</sup>	8	69	314	23

4

5 The average relative error on data is lower than 5%

6 <sup>a,b,c,d,e</sup>: values with different letters are significantly different at  $p < 0.05$  in terms of temperature

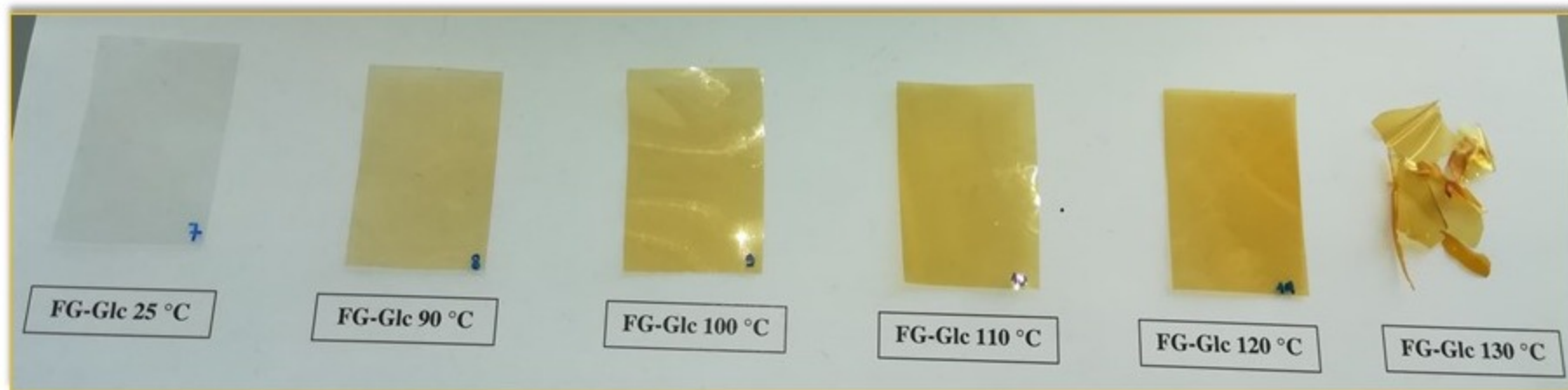
1 **Table 3:** Activation energy ( $E_a$ , kJ/mol) of GP and GP-glu films heated at different  
 2 temperatures (90 °C, 100 °C, 110 °C, 120 °C and 130 °C), with the linear regression coefficient  
 3 ( $R^2$ ).

Parameters	GP		GP-glu	
	$E_a$	$R^2$	$E_a$	$R^2$
<b>Crosslinking degree</b>	23.3	0.902	16.1	0.981
$\Delta E$	122.1	0.937	25.0	0.869
<b>Browning index</b>	-	-	40.2	0.921
<b>* Absorbance 294nm</b>	24.1 (90-120°C)	0.996	7.8	0.873
<b>* Absorbance 420nm</b>	9.7 (90-120°C)	0.940	30.1	0.980
<b>* Water solubility</b>	-8.5 (110-130°C)	0.799 <sup>NS</sup>	-1.5 (100-130°C)	0.870
<b>DPPH radical scavenging</b>	27	0.922	-22	0.759 <sup>NS</sup>
<b>ABTS<sup>+</sup> radical scavenging</b>	2.9	0.235 <sup>NS</sup>	-11	0.798 <sup>NS</sup>
<b>Reducing power</b>	45.1	0.989	1.9	0.566 <sup>NS</sup>
<b><math>\beta</math>-carotene bleaching inhibition</b>	8.8	0.672 <sup>NS</sup>	27	0.997

4  
 5 \* Arrhenius linear behavior on a limited temperature range (see Arrhenius plots in the  
 6 supplementary data)

7 <sup>NS</sup> : Non significative value of  $R^2$ , phenomena cannot be considered as an Arrhenius law's  
 8 dependence.

# Enhancement of gelatin films properties by heat treatments to favour Maillard reactions



- ↑ Crosslinking
- ↓ Solubility
- ↑ Antioxidant properties